The role of RSBN1 in mouse spermatogenesis

王, 有涛

出版情報：Kyushu University, 2022, 博士（農学）, 課程博士
バージョン：
権利関係：

The role of RSBN1 in mouse spermatogenesis

WANG YOUTAO

2021

CONTENTS

List of Abbreviation

Abbr.	Abbreviated Term
BSA	Bovine Serum Albumin
DNMT	DNA Methyltransferase
GAPDH	Glyceraldehyde-3-Phosphate Dehydrogenase
GFP	Green Fluorescent Protein
HA	Hemagglutinin
JMJD	JmjC Domain Containing Protein
KMT	Lysine (K) Methyltransferase
LSD1	Lysine Specific Demethylase 1
NLS	Nuclear Localization Signal
PFA	Paraformaldehyde
PHF8	Plant Homeodomain Finger Protein 8
PNA	Peanut Agglutinin
PRMT	Protein Arginine (R) Methyltransferase
RSBN1	Round Spermatid Basic Protein 1
WT	Wild Type

SUMMARY

During spermatogenesis, chromatin conformation of germ cells is dramatically changed and is regulated by epigenetic modifications especially methylation of histones, which contribute to differentiation of germ cells. Although the roles of Histone H3 Lysine methylation as well as methyltransferases and demethylases during spermatogenesis have been shown, the roles of Histone H4 methylation and its modifiers were rarely reported. Recently, mouse RSBN1 that has been detected to solely express in nucleus of round spermatids was identified as an ortholog of DPY-21 in *C.elegans* and a demethylase for di-methylated H4K20 (H4K20me2). To explore the dynamic change of H4K20 and the role of RSBN1 (round spermatid basic protein 1) during spermatogenesis, the localization of three different levels (mono-, di-, tri-methyl) of H4K20 and RSBN1 was studied. Immunostaining results indicated in our report that RSBN1 was not only expressed in nucleus of round spermatids but also in whole of elongated spermatids. Furthermore, the results in this study showed RSBN1 was likewise expressed in other tissues, including ovary and brain. Unlike the previous report, RSBN1 could demethylate both H4K20me3 and H4K20me2 but not H4K20me1, in RSBN1-expressed HeLa cells. I also found each methylated H4K20 was distributed in almost every stage of germ cell before spermiogenesis, although the intensity of signal is slightly different among them. Nevertheless, the intensity of each methylated H4K20 was largely different in the occurrence of spermiogenesis. Results of immunostaining indicated that tri-methylated H4K20 and di-methylated H4K20 were

significantly decreased in nucleus of round spermatids, but mono-methylated H4K20 was increased during spermiogenesis, strongly suggesting that different methylated H4K20 may play different regulatory roles in round spermatids. When the distribution pattern of RSBN1 in the seminiferous tubule was compared to that of methylated H4K20, di-methylated H4K20 and tri-methylated H4K20 but not mono-methylated H4K20 were disappeared from RSBN1 positive germ cells. Thus, these results suggested that RSBN1 could be a very important modifier to construct testis-specific landscape of methylated H4K20.

INTRODUCTION

Mouse Spermatogenesis

Spermatogenesis is the process by which spermatozoa are formed in the seminiferous tubules of the testis. This process begins with the mitotic division of spermatogonia located on the basement membrane of the tubules. Mitotic division of spermatogonia produces spermatocytes and each spermatocyte is divided into four haploid spermatids by meiosis. Finally, the round spermatids are transformed into elongated spermatids to form spermatozoa (Hess *et al.*, 2008). Generally, spermatogenesis is defined by multiple germ cells including spermatogonia, preleptotene spermatocyte, leptotene spermatocyte, zygotene spermatocyte, pachytene spermatocyte, diplotene spermatocyte, round spermatids, and elongated spermatids (Endo *et al*., 2019). Sertoli cells are somatic cells in the seminiferous tubule, are essential for the formation of histological structure of seminiferous tubules, and support development of spermatogenesis (Wu *et al*., 2021).

Chromatins of germ cells display multiple structures at different stages of spermatogenesis, which is closely connected to well-organized differentiation of germ cells. Histone modification has been reported to be a common marker of chromatins and is involved in remodeling of chromosomal conformation and regulating gene expression (Brejc *et al*., 2017; Kumari *et al*., 2020; Wells *et al.,* 2012).

Histone methylation.

Nucleosome is the core structure of chromatin. Each nucleosome consists of approximately 146 bp of double-strand DNA wrapped around a histone octamer, which consists of two copies of four histone proteins: H2A, H2B, H3 and H4 (Mohan *et al*., 2021; Redon *et al*., 2002; Stillman *et al*., 2018). N-terminus of each histone proteins can be modified by some chemical groups, such as acetyl group (acetylation), methyl group (methylation), and so on. Several lysines (K) of H3 and H4, such as H3K4, H3K9, H3K27, H3K36, H4K20, can be methylated into three status: mono-methylation (me1), di-methylation (me2) and tri-methylation (me3). Each lysine methylated H3 or H4 plays a vital role in modulating chromatin structure and affecting transcriptional regulation activity (Huang *et al*., 2015). For example, methylation on H3K4 and H3K36 promote transcription, whereas methylation on H3K9, H3K27 and H4K20 inhibit transcription (Bannister *et al*., 2011; Greer *et al*., 2012; Iwamori *et al*., 2013; Jørgensen *et al*., 2013; Kouzarides *et al*., 2007; Martin *et al*., 2005; Peters *et al*., 2001).

Among these methylated histones, methylated H4K20 has unique characteristics to oscillate during the cell cycle and multiple functions other than transcriptional repression. Methylated H4K20 is critical for genome integrity including DNA damage repair, DNA replication, chromatin compaction, and so on (Jørgensen *et al*., 2013; Pei *et al*., 2011; Schotta *et al*., 2004; Shoaib *et al*., 2018; Wang *et al*., 2009). Although the distributions of methylated H4K20 during spermatogenesis was already shown (Payne *et al*., 2006; Shirakata *et al*., 2014), little is known about the role of methylated H4K20 during germ cell differentiation.

Histone demethylases

Histone methylation is regulated by methyltransferases and demethylases (Morera *et al*., 2016; Mosammaparast *et al*., 2010; Walport *et al*., 2012). To date, at least three demethylases (PHF8/KDM7B, LSD1n, and RSBN1/KDM9) directly regulate H4K20 methylation (Brejc *et al*., 2017; Liu *et al*., 2010; Qi *et al*., 2010; Wang *et al*., 2015). PHF8 and LSD1n can demethylate mono-methylated H4K20, while RSBN1 can demethylate di-methylated H4K20. Recently, human hHR23, a new histone demethylase for methylated H4K20 was identified. It could demethylate tri-, di-, and mono-methylated H4K20 and hHR23B-deficient mice showed impaired embryonic development (Cao *et al*., 2020; Ng *et al*., 2002).

To date, the roles of demethylase for methylation of H4K20 during mouse spermatogenesis still remain to be elucidated. Previous report indicated that the expression of round spermatids basic protein 1 (RSBN1/KDM9) was testis-specific (Takahashi *et al*., 2004). In addition, partial amino acids of RSBN1 ($RSBN1^{350-795}$) could convert H4K20me2 to H4K20me1 but could not catalyze the demethylation of H4K20me3 (Brejc *et al*., 2017). However, the role of RSBN1 during spermatogenesis remains unclear.

Organization of this thesis

In the chapter I, expression of RSBN1 in multiple tissues was examined by semiquantitative PCR. Then, a newly developed RSBN1 polyclonal antibody was purified, and its antibody specificity was evaluated by *in vitro* experiments. After that,

localizations of RSBN1 in testis and ovary were examined by immunofluorescence microscopy using the purified antibody.

In chapter II, distributions of mono-methylated H4K20, di-methylated H4K20, and tri-methylated H4K20 in the seminiferous tubules were examined at different stages of spermatogenesis by immunostaining.

In chapter III, demethylation function of RSBN1 on methylated H4K20 was verified by immunoblotting and immunostaining. Additionally, distribution of RSBN1 and methylated H4K20 were compared at stage VII in spermatogenesis.

CHAPTER I

Expression of RSBN1 in different tissues and RSBN1 localization in spermatogenesis.

Introduction

Spermiogenesis, the final stage of spermatogenesis, begins with haploid round spermatids that undergo a series of complex changes, including acrosome formation, chromatin compaction, tail formation, and phagocytosis. During these processes, round spermatids transform into elongated spermatids that further develop into mature spermatozoa (Nishimura *et al*., 2017). During spermiogenesis, germ cell differentiation is regulated by different proteins that are temporarily or continuously expressed. These factors are related to transcriptional regulation or chromosome remodeling of haploid germ cells (Blendy *et al*., 1996; Luense *et al*., 2019; Nantel *et al*., 1996).

Round spermatid basic protein 1 (RSBN1) was first reported in 2004 (Takahashi *et al*., 2004). The full-length sequence was 2,388 bp, which encodes 795 amino acids. In the previous study, RSBN1 cDNA was isolated by subtracting the cDNA of 17-day-old testes from 35-day-old mouse testes cDNA. Previous findings also have demonstrated that RSBN1 is exclusively expressed in the testis, but not in other tissues. However, information from GenBank indicates that RSBN1 is expressed not only in the testis, but also in the brain and ovary, which is inconsistent with the previous results.

To explore the role of RSBN1 in spermatogenesis, it is necessary to confirm its localization and expression in the testes.

Here, reverse transcription polymerase chain reaction (RT-PCR) was performed to show the RSBN1 expression in several tissues. In addition, a newly designed antibody was used for western blot analysis to confirm RSBN1 protein expression in reproductive tissues.

Materials and Methods

Semiquantitative RT-PCR

Total RNA of twelve different tissues were extracted by ISOGEN II (Nippon Gene), followed by reverse transcription using PrimeScript II RTase and random primer (Takara). The primers to amplify *Rsbn1* cDNA fragment spanning exons 8 and 9 were as follows: forward, 5'-AGTGAAAATGAGAAAAACGC-3'; reverse, 5'-CACAGGA GTGCTTGGATGTG-3'.

Nuclear Localization Signal (NLS) prediction

In this study, the putative nuclear localization signals (NLS) in RSBN1 were predicted by NLS Mapper (https://nls-mapper.iab.keio.ac.jp/cgi-bin/ NLS_Mapper_ form.cgi).

Polyclonal Antibody

An antibody against mouse RSBN1 was developed in a rabbit by an immunization using the RSBN1 specific peptide (SCRUM Inc.). The sequence of RSBN1 specific peptide is as follows: Cys-ETAQNTESNSNM. The polyclonal antibody was purified from rabbit serum by affinity chromatography using an antigen peptide.

Cell culture and Transfection

The open reading frame (ORF) sequences of mouse RSBN1 was subcloned into

pCS2-F vector, which contains a C-terminal FLAG tag sequence, by In-fusion HD cloning kit (Takara) according to the manufacturer's instruction. The primer sequences that are used to amplify the vector and RSBN1 were listed in Table 1. HEK-293T and Hela cells were maintained in Dulbecco's modified Eagle Medium (Thermo Scientific) supplemented with 10% fetal calf serum (SIGMA), 1% glutamine (Wako), and 1% penicillin-streptomycin (Wako) at 37˚C in a humidified 5% CO_2 atmosphere in air. The cells were transfected using Screen*F*ect^{TM} A *plus* (Wako) following manufacturer's instruction. The transfected Hela cells were cultured for 48 hours and re-seeded onto poly-L-lysine coated coverslips, followed by immunostaining analysis. Here, the HEK-293T cells were used for sample preparation of western blot.

Western Blot

To detect RSBN1 protein in multiple tissues or culture cells, RIPA lysis buffer (10mM Tris-HCl [PH7.4], 150mM NaCl, 0.5M EDTA, 1% NP-40, 0.1% SDS) was utilized to prepare tissue lysate samples and cell lysates. Primary Antibodies used are anti-RSBN1 (SCRUM Inc.), anti-Beta Actin (Abcam), anti-Flag (Wako). Secondary antibodies are as follows: Goat anti-rabbit IgG-HRP and Goat anti-mouse IgG-HRP (both from Bio-Rad).

Immunofluorescence

Mouse testes or ovaries were fixed in 4% paraformaldehyde (PFA) for 48 hours, followed by infiltration in 30% sucrose solution for overnight, and then they were

embedded in OCT compound (Sakura Finetek USA, Inc.) and frozen by liquid nitrogen. For Hela cells, they were fixed by PFA at room temperature for 30 min. Frozen sections (6μm thickness) were cut and placed on adhesive glass slides. After rinsed in PBS and permeabilization with 0.5% triton X-100, tissue sections or Hela cells were blocked in 3% bovine serum albumin (BSA)-PBS for one hour at room temperature. Then, samples were incubated with the primary antibodies, which were diluted 1:1,000 with 3% BSA-PBS blocking buffer, for overnight at 4˚C, followed by incubation with the secondary antibodies for one hour at room temperature. Primary antibodies used in this study were anti-RSBN1 polyclonal antibody (SCRUM Inc.) and anti-Flag antibody (Wako). An absorbed antibody was used as a control staining. Secondary antibodies were Alexa 555-conjugated donkey anti-rabbit IgG and Alexa 488-conjugated goat anti-mouse (Both from Invitrogen). The samples were examined by fluorescence microscopy after nucleus staining with Hoechst 33342 (Invitrogen) and acrosome staining with PNA-FITC (Jackson Immunores).

Results and Discussion

To examine RSBN1 expression in mice, twelve tissues were collected from adult mice. These tissues included samples from brain, heart, lungs, kidney, intestine, liver, pancreas, spleen, muscle, limbs, ovary, and testis. RT-PCR results suggested that *Rsbn1* mRNA was detected not only in testis but also in other tissues. RSBN1 was expressed at high levels in testis and brain; at moderate levels in heart, lung, liver, and ovary; and at a low level in limb (Fig 1), indicating that RSBN1 is not exclusively expressed in the testis. mRNA of *Rsbn1* in testis was reverse transcribed to synthesize cDNA, then the RSBN1 ORF was subcloned into pCS2-F for construction of recombinant plasmid pCS2-RSBN1-Flag (Fig 2) for transfection into HeLa cells and 293T cells. In this study, a newly designed antibody against RSBN1 was developed in a rabbit and purified from rabbit serum using affinity chromatography. Antibody specificity was evaluated by immunoblotting and immunostaining after RSBN1 was expressed in HeLa cells and 293T cells. Immunoblotting analysis suggested that a single band in each lane was recognized by RSBN1 polyclonal antibody and Flag monoclonal antibody (Fig 3A). Furthermore, immunostainings showed that the fusion proteins expressed in HeLa cells were restricted to the nucleus and that the signal intensity in each HeLa cell stained using the two types of antibodies overlapped thoroughly (Fig 3B). The data indicated that the newly developed polyclonal antibody could specifically recognize RSBN1 protein.

To further determine the expression of RSBN1 protein, six tissue lysates in which

Rsbn1 mRNA was detected were analyzed by immunoblotting, resulting in the identification of RSBN1 expression in testis, brain, and ovary, but not in liver, heart, or lung (Fig 4). The results implied that RSBN1 may be involved in the development and/or regulation of both brain and germ cells. A previous study indicated that RSBN1 is exclusively located in round spermatids (Takahashi *et al*., 2004). Its distribution in the seminiferous tubules was examined using the newly developed antibody against RSBN1. Immunofluorescent staining of testis sections indicated that RSBN1 protein signals were mainly detected in the nucleus of round spermatids and in both the nucleus and cytoplasm of elongated spermatids. Nevertheless, the intensity of RSBN1 immunosignals in round spermatids was very weak, and the intensity of those in elongated spermatids was very strong (Fig 5A). Unexpectedly, RSBN1 signals in the ovary were not detected in germ cells but were concentrated in the cytoplasm of stromal cells (Fig 5B).

Compared with previous report, our results revealed some differences. Firstly, RSBN1 was only expressed in the testes in the previous study, whereas RSBN1 was expressed in brain, testis, and ovary, based on our results. Although it is difficult to explain the reasons for this difference, the methods employed may be able to explain such differences. Northern blotting and RT-PCR were utilized in the previous study and in our study, respectively. Since RT-PCR has greater sensitivity than northern blot analysis, weak expressions of *Rsbn1* in other tissues could be detected by RT-PCR. The second difference was the localization of RSBN1 in the seminiferous tubules. As suggested in the previous report, RSBN1 is localized in the nuclei of round spermatids.

However, our immunostaining analysis showed that RSBN1 was detectable not only in round spermatids but also elongated spermatids. This difference can be explained by differences in the antibodies used in the two analyses. A fragment of a RSBN1 peptide sequence (ETAQNTESNSNM, residues 709-720) was utilized in our study, whereas a different peptide fragment (VFKVESRLDSDQQH, residues 772–785) was used for immunization in the previous study. In addition, testis sections were fixed with 4% paraformaldehyde (PFA) in this study, whereas they were fixed with 100% ethanol in the previous report. This experimental difference could lead to distinct results because of the different effects of PFA and ethanol fixation on antigens.

RSBN1 was localized in the nucleus of round spermatids, whereas it is localized in both the nucleus and the cytoplasm of elongating spermatids (Fig 5A). Since there were three putative nuclear localization signals (NLSs) found in RSBN1 (Fig 6), RSBN1 in the cytoplasm of elongated spermatids could be interacted with and retained by other proteins that play a role in the cytoplasm of elongating spermatids. To date, only a small number of studies have suggested the role of histone demethylases in the cytoplasm of maturing spermatids. KDM3A/JHDM2A is localized in the cytoplasm of elongating spermatids, and deficiency of KDM3A leads to deformed acrosomes, incomplete manchettes, and detached centrosomes (Kasioulis *et al*., 2014). Furthermore, the interaction between KDM3A and HSP90 in the cytoplasm of maturing spermatids is essential for cytoskeletal rearrangements during spermiogenesis (Kasioulis *et al*., 2014). Since RSBN1 was also expressed in the cytoplasm of maturing spermatids, it could be necessary to identify proteins that interact with RSBN1 to investigate a role

of RSBN1 in the cytoplasm of elongating spermatids as well as to explore whether RSBN1 is involved in the cytoskeletal rearrangements of spermatids.

Although the localization of RSBN1 in the ovary was identified in the present study, RSBN1 was not localized in female germ cells. Immunostaining showed that RSBN1 signals were intense in the cytoplasm of stromal cells surrounding follicles. Stromal cells play an essential role in follicular development. For example, they can multiply and differentiate into thecal cells to maintain integrity of the follicle structure and outer myofibroblasts, which secrete extracellular matrix, including type I and type III collagen fibers (Jiang *et al*., 2003). Furthermore, the outer tissues of the follicles can promote the formation of follicular capillaries, which provide nutrients for follicle growth and development (Wang *et al*., 2001). Thus, stromal cells are essential for follicle development. In a recent report, RSBN1 expression in the mouse ovary was reported to be regulated by miR-378d in vitamin D (VD)-deficient mice, which is associated with the expression of GLUT4, and GLUT4 is responsible for insulin-stimulated glucose uptake (Sun *et al*., 2021). VD promotes the production of hormones and growth factors, including estradiol, estrone, progesterone, and insulin-like growth factor-binding protein 1 in the ovary. These hormones and growth factors are critical for follicular and embryonic development (Parikh *et al*., 2010). VD could also correct reproductive dysfunction in female mice, and RNA-sequencing analysis showed that RSBN1 expression decreases in VD-deficient ovaries (Sun *et al*., 2021). Another study indicated that RSBN1 is associated with the expression of anti-Mullerian hormone (AMH) and the production of steroid hormones, which regulate follicle formation

(Ohyama *et al*., 2015). Moreover, VD directly targets AMH in vivo, and AMH mRNA expression is upregulated in response to vitamin D in fertile females (Lata *et al*., 2017). Thus, RSBN1 in stromal cells may play a positive role in follicle development.

Table. 1. Primer sequences used for construction of recombinant plasmid in this study.

Name	Forward Primer	Reverse Primer
RSBN1	TCAAGGCCTCTCGAGATGTTCAGGTCTA CGAGAACGAC	GTCGTCCTTGTAGTCCACAGGAGTGCTTGGATGTG
pCS2-F	GACTACAAGGACGACGATGACA	CTCGAGAGGCCTTGAATTCA

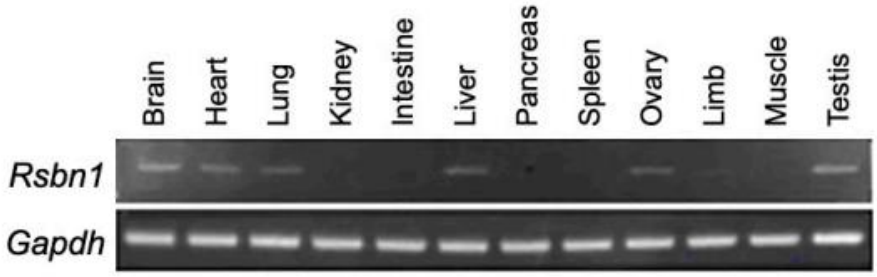

Fig. 1. Expression of *Rsbn1* in multiple tissues. Transcripts of *Rsbn1* were examined by semiquantitative RT-PCR in different tissue samples. *Gapdh* was used as an internal control.

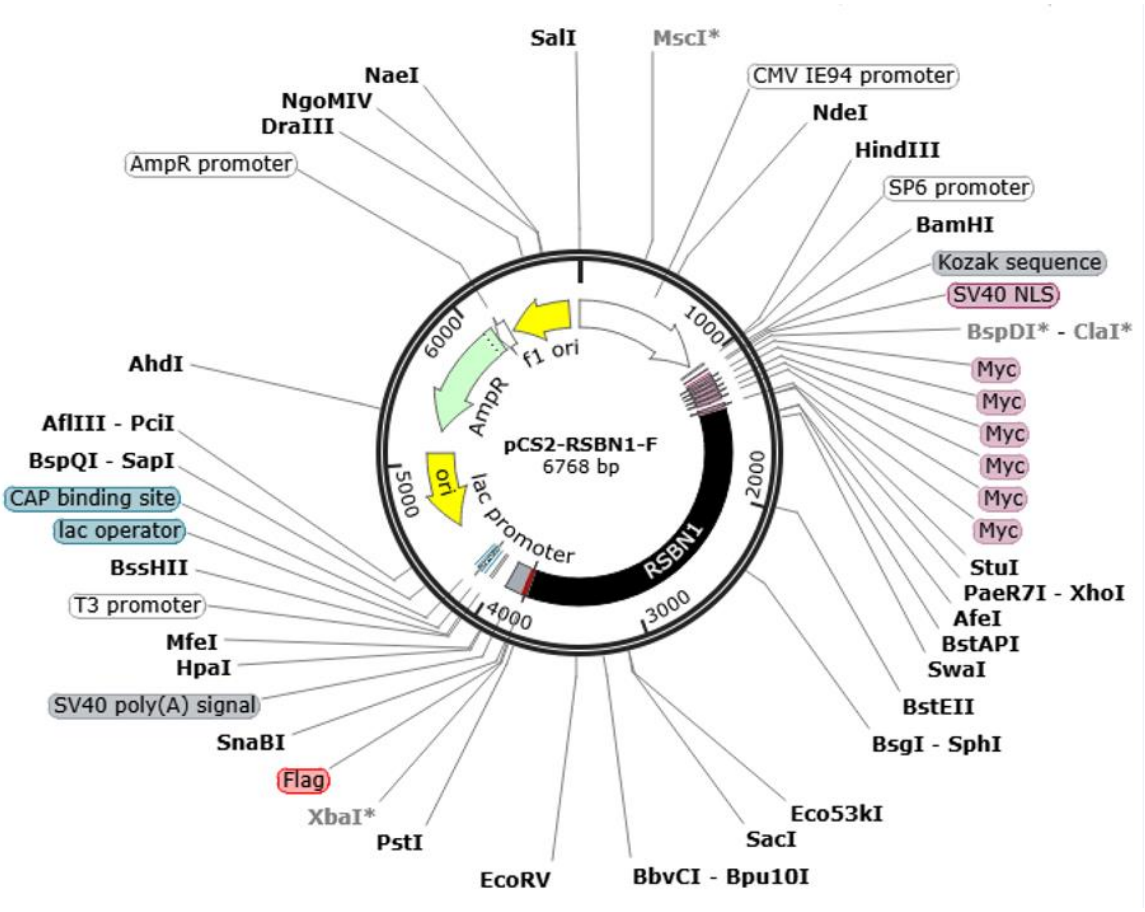

Fig. 2. Information of recombinant plasmid pCS2-RSBN1-Flag. ORF of RSBN1 was subcloned into pCS2-F vector by in-fusion HD cloning kit.

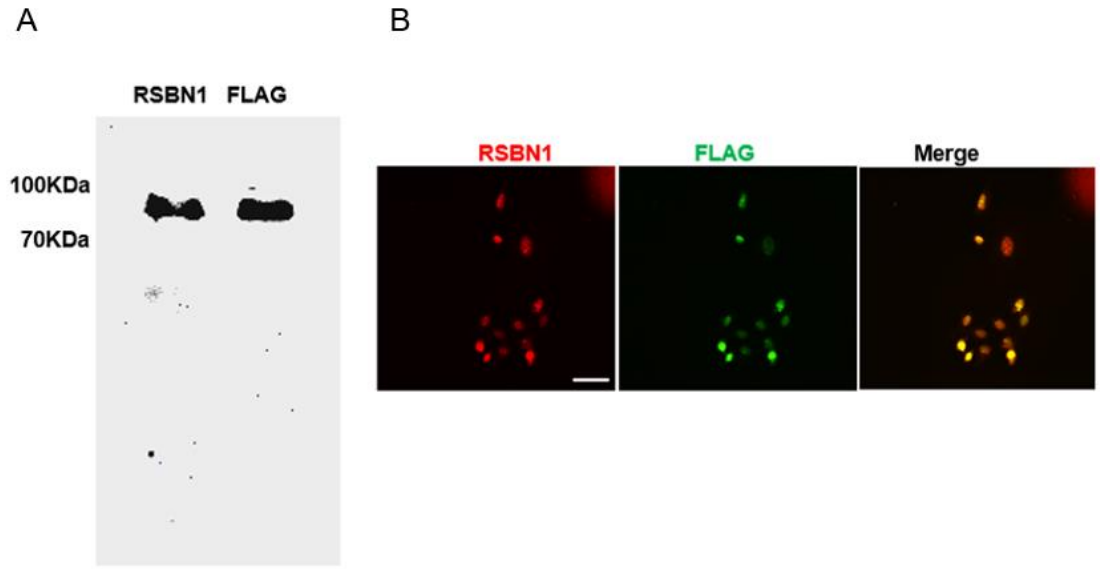

Fig. 3. Evaluation of the specificity of the RSBN1 antibody. (A) A representative immunoblotting result to detect FLAG-Tagged RSBN1 protein expressed in 293T cells using the anti-RSBN1 and the anti-FLAG antibodies. The molecular weight of RSBN1 is about 90 kDa. (B) The immunostaining evaluation of the specificity of the RSBN1 antibody. Transfected HeLa cells were double stained by the antibodies against RSBN1 and FLAG. Representative immunofluorescent images of RSBN1 (red) and FLAG (green) in FLAG-RSBN1 expressed HeLa cells are shown. Scale bar = 20μm.

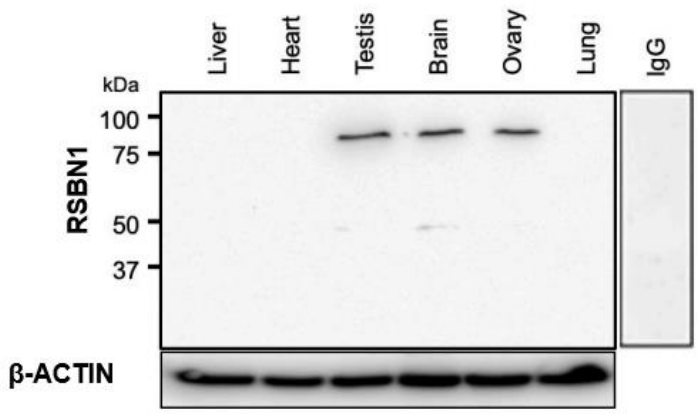

Fig. 4. Expression of RSBN1 protein in multiple tissues. A immunoblot results of RSBN1 protein in six different tissues are shown. Mouse IgG was used for negative control. Beta-actin was used as an internal control.

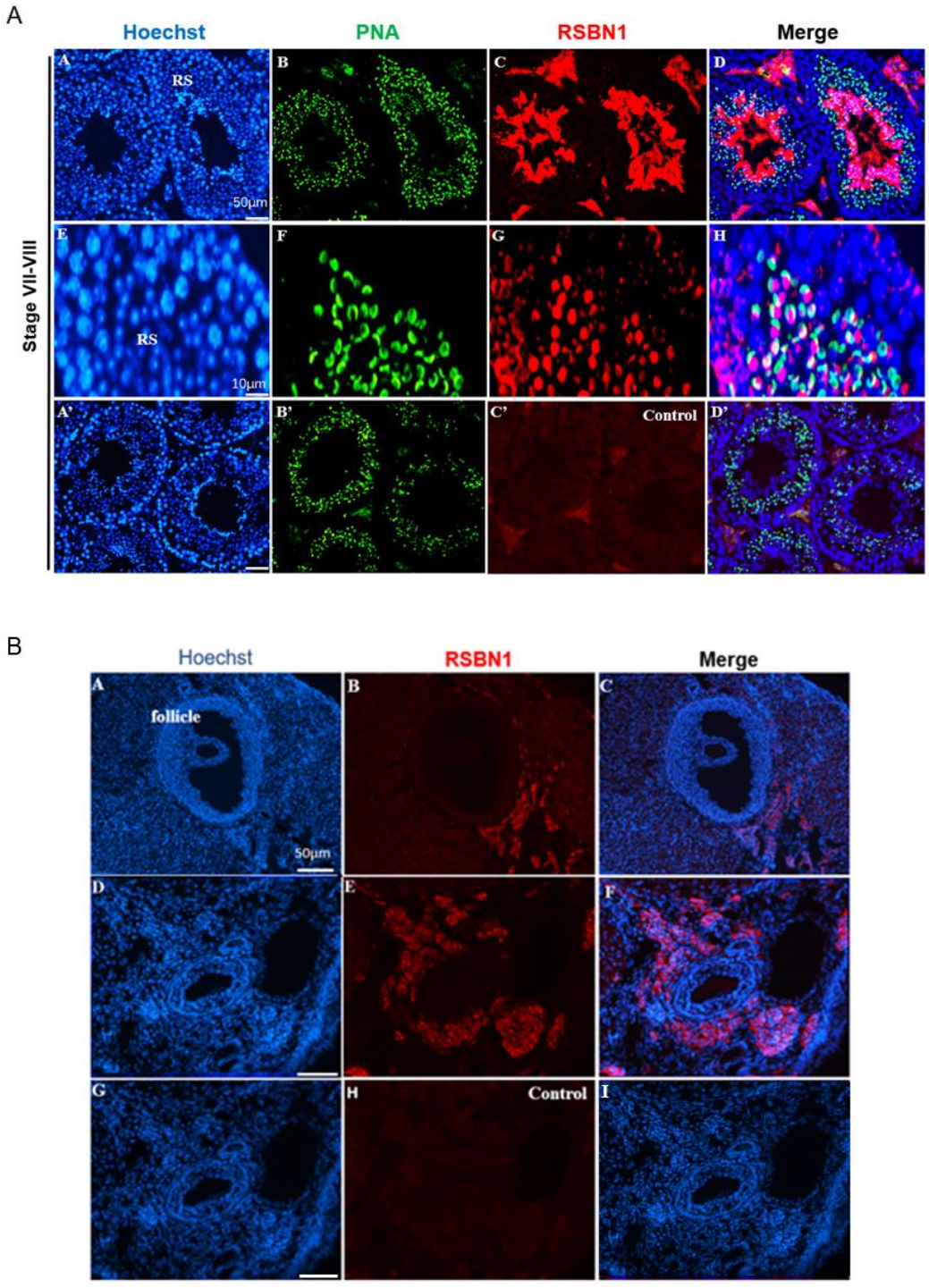

Fig. 5. Localization of RSBN1 in the testis and the ovary. (A) The localizations of nucleus (Hoechst, blue: A, E, and A'), acrosome (PNA, green: B, F, and B'), RSBN1 (red: C and G), an absorbed antibody used as a control (C'), and merged images (D, H, and D') in the seminiferous tubules are shown. RS, round spermatids. ES, elongated

spermatids. Scale bars = 50μm (A-D, A'-D') and 10μm (E-H). (B) The localization of nucleus (Hoechst, blue: A, D, and G), RSBN1 (red, B and E), an absorbed antibody used as a control (H), and merged images (C, F, and I) in the ovary are shown. Scale bars = 50μm (A-I).

A

MFRSTRTTDQWRVGERLQCPAGHARAALARTADGGAVGPFKCVFVGEMAAQVGAVRVVRAV
AAQEEPDKEGKEKPHVGVSPRGVKRQRRASSGGSQEKRGRPSQDPPLAPPHRRRRSRQHPGPLP
PTNAAPTVPGPVEPLLLPPPPPPSLAPAGPTVAAPLPAPGTSALFTFSPLTVSAAGPKHKGHKERH
KHHHHRGSDGDPGACVPGDLKHKDKQENGERSGGVPLIKAPKRETADENGKTQRADDFVLKK
IKKKKKKKHREDMRGRRLKMYNKEVQTVCAGLTRISKEILTQGQLNSTSGVNKESFRYLKDEQL
CRLNLGMQEYRVPQGVQTPFTTHQEHSIRRNFLKTGTKFSNFIHEEHQSNGGALVLHAYMDELS
FLSPMEMERFSEEFLALTFSENEKNAAYYALAIVHGAAAYLPDFLDYFAFNFPNTPVKMEILGKK
DIETTTISNFHTQVNRTYCCGTYRAGPMRQISLVGAVDEEVGDYFPEFLDMLEESPFLKMTLPW
GTLSSLQLQCRSQSDDGPIMWVRPGEQMIPTADMPKSPFKRRRSMNEIKNLQYLPRTSEPREVLF
EDRTRAHADHVGQGFDWQSTAAVGVLKAVQFGEWSDQPRITKDVICFHAEDFTDVVQRLQLD
LHEPPVSQCVQWVDEAKLNQMRREGIRYARIQLCDNDIYFIPRNVIHQFKTVSAVCSLAWHIRL
KQYHPVVETAQNTESNSNMDCGLEVDSQCVRIKTESEERCTEMQLLTTASPSFPPPSELHLQ
DLKTQPLPVFKVESRLDSDQQHSLQAHPSTPV

B

Position	Sequence
81-117	PRGVKRQRRASSGGSQEKRGRPSQDPPLAPPHRRRRS
254-265	IKKKKKKKHRED
547-557	SPFKRRRSMNE

Fig. 6. Prediction of NLS sequences in RSBN1. (A) Locations of putative NLS sequences in mouse RSBN1. Full amino acids of RSBN1 and predicted NLS sequences (red) are shown. (B) Amino acid sequences of putative NLS. Amino acid sequences of three putative NLSs and their positions are listed.

CHAPTER II

The distribution of mono-methylation, di-methylation, and tri-methylation of histone H4 lysine 20 during spermatogenesis.

Introduction

Among several methylated histones, methylated H4K20 has multiple functions and the function of methylated H4K20 is varied among methylated degree (Wang *et al*., 2009). For example, recognition of H4K20me1 by L3MBTL1 promotes chromatin compaction and transcriptional repression (Beck *et al*., 2012). Furthermore, H4K20me1 has been shown to promote X-chromosome compaction in *C. elegans* dosage compensation as well as marks the initiation of X-chromosome inactivation in mouse undifferentiated ES cells (Brejc *et al*., 2017; Fang *et al.*, 2002; Kalakonda *et al*., 2008; Kohlmaier *et al*., 2004). H4K20me3 is required to ensure positive replication of heterochromatin in human U2OS cells, and it acts as an important repressive marker (Brustel *et al*., 2017; Schotta *et al*., 2004; Schotta *et al*., 2008). Although methylated H4K20 during spermatogenesis was shown (Shirakata *et al*., 2014), how each methylated H4K20 contributes to differentiation of germ cells remain to be elucidated.

In the present study, dynamic distribution involving methylated H4K20 at different

stages of spermatogenesis were investigated. I found that the distribution of H4K20 methylation at different stages of spermatogenesis was variable. Three methylated H4K20 were distributed at most stages of spermatogenesis, while the distinct distribution pattern of three types of methylated H4K20 was dependent on stages of spermatogenesis and could be related with chromatin compaction as well as transcription in germ cells.

Materials and Methods

Immunofluorescence

Mouse testes were fixed in 4% paraformaldehyde (PFA) for 48 hours, followed by infiltration in 30% sucrose for overnight, then testes were embedded by OCT compound (Sakura Finetek USA, Inc.) and frozen by liquid nitrogen. Frozen sections (6μm sickness) were cut and placed on adhesive glass slides. After rinsed in PBS and permeabilization with 0.5% triton X-100, sections were blocked in 3% bovine serum albumin (BSA)-PBS for one hour at room temperature. Then, sections were incubated with primary antibodies diluted 1:1000 with 3% BSA-PBS blocking buffer, for overnight at 4˚C and followed by incubation with secondary antibodies for one hour at room temperature. Primary antibodies used in in this study were as follows, mouse anti-H4K20me1 (GeneTex); mouse anti-H4K20me2 (GeneTex); mouse anti-H4K20me3 (Abcam) monoclonal antibody. Secondary antibody was Alexa 488-conjugated goat anti-mouse IgG (Invitrogen). The frozen sections were examined by fluorescence microscopy after nuclear staining with Hoechst 33342 (Invitrogen). Stages of the seminiferous epithelium were determined by nucleus staining.

Results and Discussion

To determine the distribution of methylated H4K20, H4K20 methylation was examined by immunofluorescent staining at several stages of spermatogenesis. Generally, there are 12 stages (I ~ XII) involved in mouse spermatogenesis and 16 steps for spermiogenesis (Russell *et al*., 1990) (Fig 1), and I focused on changes in H4K20 methylation at stages I, VIII, IX-X, and XI-XII. The results indicated that H4K20me3 fluorescence intensity was strong in pachytene spermatocytes but weak in round and elongated spermatids at stage I (Fig 2). At stage VIII, the H4K20me3 signal remained strong in pachytene spermatocytes and preleptotene spermatocytes but was still weak in spermatids (Fig 2). At stages IX and X, H4K20me3 was weak in pachytene spermatocytes but strong in leptotene spermatocytes (Fig 2). At the final stage (XII), H4K20me3 was strong in zygotene spermatocytes and was moderately accumulated during meiosis (Fig 2). H4K20me3 is a hallmark of repressed chromatin in eukaryotes and maternal pericentric regions (Balakrishnan *et al*., 2010; Probst *et al*., 2007). In the present study, the intensity of H4K20me3 staining changed in pachytene spermatocytes at stages I, VIII, IX, and X, suggesting that it maintains heterochromatin and could repress transcription in pachytene spermatocytes. Furthermore, the overall H4K20me3 distribution in different male germ cells might also be related to paternal genomic imprinting because H4K20me3 has been detected in paternally methylated imprinting control regions (ICRs) and marks ICRs during spermatogenesis (Delaval *et al*., 2007). Also, it is likely that H4K20m3 regulate the telomere length in the germ cells, since

H4K20me3 is enriched in the telomeric and subtelomeric domains and since relative telomere length is dynamically changed during spermatogenesis (Benetti *et al.*, 2007; Fice *et al*., 2019; Ozturk *et al*., 2015; Tanemura *et al*., 2005). At least, it is possible that H4K20me3 demethylation occurs in germ cells during post-meiotic stages, since a strong H4K20me3 signal was not found at these stages.

Similarly, H4K20me2 signal intensity was strong in pachytene spermatocytes but weak in round spermatids and elongated spermatids at stage I (Fig 3). The H4K20me2 signal was weaker in round spermatids at stage VIII than in stage I spermatids, but it remained strong in the nuclei of pachytene, preleptotene, and leptotene spermatocytes (Fig 3). At stages XI-XII, the H4K20me2 signal was weak in zygotene spermatocytes, but strong during meiosis (Fig 3). To date, there have been few reports regarding the correlation between H4K20me2 and transcription in animals. Some studies have suggested that H4K20me2 is involved in DNA damage repair. For example, methyltransferase MMSET-mediated H4K20me2 significantly accumulates at sites of double-strand breaks (DSBs) in HeLa cells (Pei *et al*., 2011). The checkpoint protein Crb2 preferentially binds to the H4K20me2 residue at genomic lesions in yeast, which is very important for maintaining genome stability of the fission yeast *Schizosaccharomyces pombe* (Greeson *et al*., 2008). In this study, H4K20me2 was strong in pachytene spermatocytes but disappeared at the post-meiotic stage, so that H4K20me2 in pachytene spermatocyte could be related to DNA repair. In mouse spermatocytes, endogenous DSBs are introduced by the endonuclease SPO11, which contributes to homologous chromosome recognition and is repaired by homologous

recombination (HR) at the first meiotic prophase (Ahmed *et al*., 2021; Paquin *et al*., 2018). In addition, BRCA1, a binding protein of H4K20me2, promotes HR by activating DNA end resection (Isono *et al*., 2017). Thus, it is possible that H4K20me2 is largely recruited during HR and is involved in the repair of DSBs by HR. It remains to be studied whether it is associated with other functions, such as gene transcription or chromatin organization.

H4K20me1 distribution was different from the distribution of H4K20me3 and H4K20me2 at the same stages of spermatogenesis. The signal intensity of H4K20me1 was very strong in round spermatids, but medium in pachytene spermatocytes at stage I (Fig 4). H4K20me1 intensity was also strong in round spermatids and pachytene spermatocytes, whereas it was weak in both elongated spermatids and preleptotene spermatocytes at stage VIII (Fig 4). The H4K20me1 signal in leptotene spermatocytes was also weak at stages IX and X, whereas it was very strong in elongated spermatids at these two stages (Fig 4). At the stages XI and XII, H4K20me1 was strong in zygotene spermatocytes (Fig 4). Overall, H4K20me1 was enriched in the chromocenter of spermatids at stages I-VIII, unlike H4K20me2 and H4K20me3, which were decreased at these stages. When round spermatids transform into elongated spermatids during spermiogenesis, chromatin undergoes condensation and structural remodeling. Therefore, enrichment of H4K20me1 could contribute to the alteration of haploid spermatid chromatin conformation in the steps 1-10 of spermiogenesis.

Previous studies have reported that H4K20me1 is a repressed marker in both prokaryotic and eukaryotic cells, which can drive the compaction of chromatin, and

thus, maintain genome integrity (Brejc *et al*., 2017; Karachentsev *et al*., 2005; Shoaib *et al*., 2018; Tjalsma *et al*., 2021). At stages IX and X, immunostaining suggested that H4K20me1 was strongly accumulated in spermatids, in which chromatins are compacted into the head of spermatozoa. Additionally, H4K5ac, H4K8ac, and H4K12ac at these two stages are also intensive and could increase chromatin relaxation (Luense *et al*., 2019). Therefore, histone H4 bearing different types of modification at post-meiotic stages. In contrast to the function of histone acetylation, H4K20me1 can maintain the integrity of genome. For example, SET8-dependent accumulation of H4K20me1 not only promotes the compaction of chromatin, which is essential for genome integrity during mitosis in U2OS cells, but also plays a role in inhibiting aberrant unwinding of DNA by limiting chromatin-associated pre-replicative complex components in U2OS cells during the G1 phase (Shoaib *et al*., 2018). Thus, it is possible that the effect of histone H4K20me1 on the chromatin strike a balance with that of histone acetylation at the stages of IX and X to maintain the higher-order chromosome structure. Therefore, H4K20me1 at the stages IX-X in spermatogenesis could limit excessive relaxation of chromatin and maintain the orderly conformation of chromatin.

Since the degree of enrichment of H4K20me1 at the spermiogenesis stage is much higher than that of di- and tri-methylated H4K20, it is obvious that H4K20 mono-methylation is an important marker at the post-meiotic stages of spermatogenesis. However, it remains unclear whether its effects on gene transcription are achieved by co-acting with other factors in the promoter region or by changing chromatin conformation directly. It is necessary to perform ChIP-seq to provide a novel annotation

of H4K20me1 in spermiogenesis. Consequently, the specific function of mono-methylated H4K20 during spermiogenesis requires further investigation.

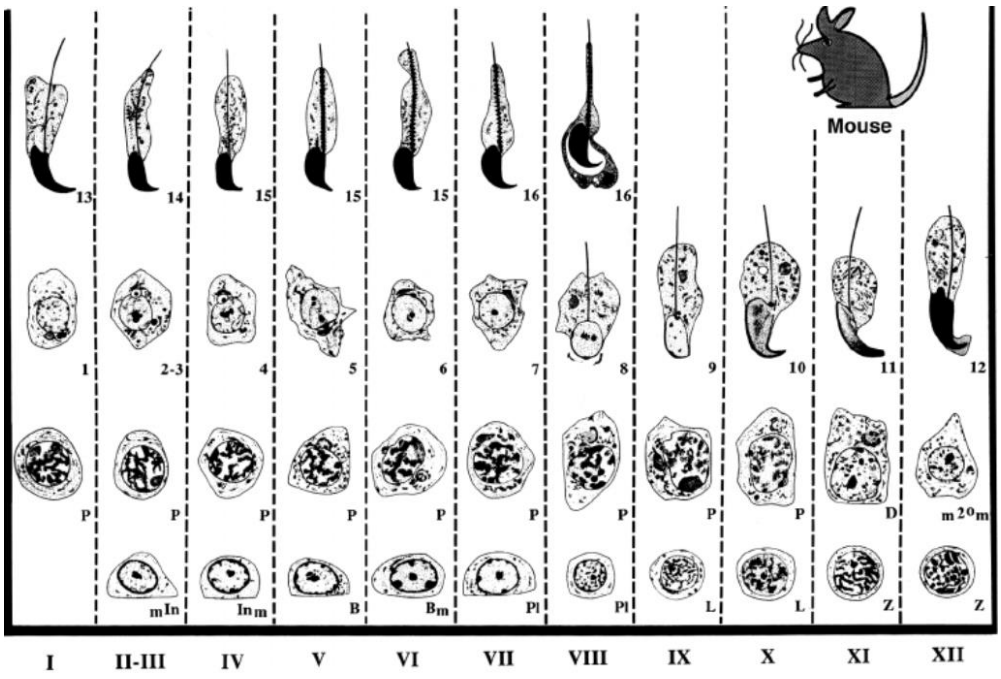

Fig. 1. Stages of spermatogenesis and steps of spermiogenesis to produce spermatozoa in the mouse seminiferous tubules. The abscissa Roman numerals depict the stages of spermatogenesis, while the Arabic numbers depict the steps of spermiogenesis. Several types of cell are shown: type A spermatogonia in mitosis (m^{In}), intermediate spermatogonia in mitosis (In_m), type B spermatogonia (B), type B spermatogonia in mitosis (B_m), preleptotene spermatocyte (Pl), leptotene spermatocyte (L), zygotene spermatocyte (Z), pachytene spermatocyte (P), diplotene spermatocytes (D) and secondary spermatocytes in meiosis (m2°m) (Russell *et al*., 1990).

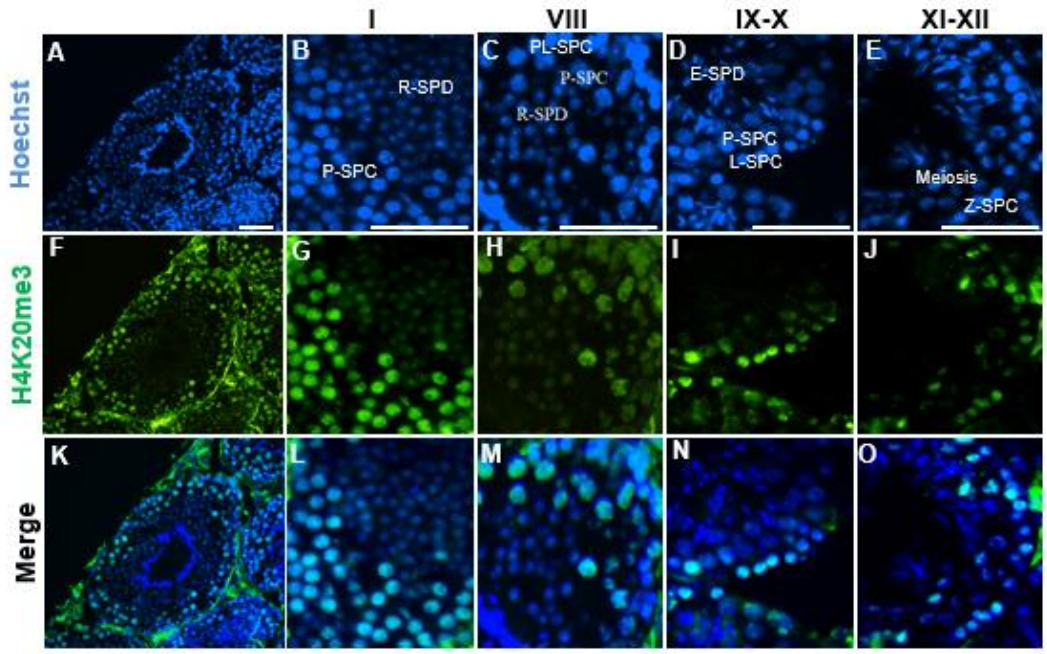

Fig. 2. The distribution of tri-methylated H4K20 in the seminiferous tubules. The distributions of nucleus (Blue: A-E), H4K20me3 (Green: F-J), and merged images (bottom panel: K-O) at stages I, VIII, IX-X, and XI-XII are shown. PL-SPC, preleptotene spermatocyte; L-SPC, leptotene spermatocyte; Z-SPC, zygotene spermatocyte; P-SPC, pachytene spermatocyte; R-SPD, round spermatid; E-SPD, elongated spermatid. Scale bars = 20μm.

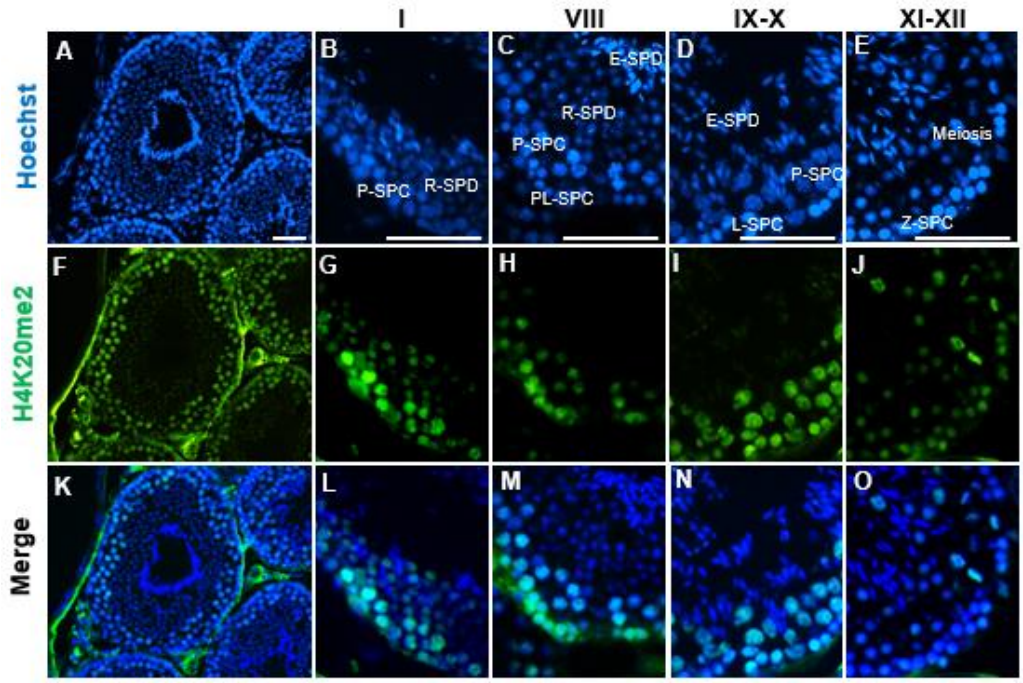

Fig. 3. The distribution of di-methylated H4K20 in the seminiferous tubules. The distributions of nucleus (Blue: A-E), H4K20me2 (Green: F-J), and merged images (bottom panel: K-O) at stages I, VIII, IX-X, and XI-XII are shown. PL-SPC, preleptotene spermatocyte; L-SPC, leptotene spermatocyte; Z-SPC, zygotene spermatocyte; P-SPC, pachytene spermatocyte; R-SPD, round spermatid; E-SPD, elongated spermatid. Scale bars = 20μm.

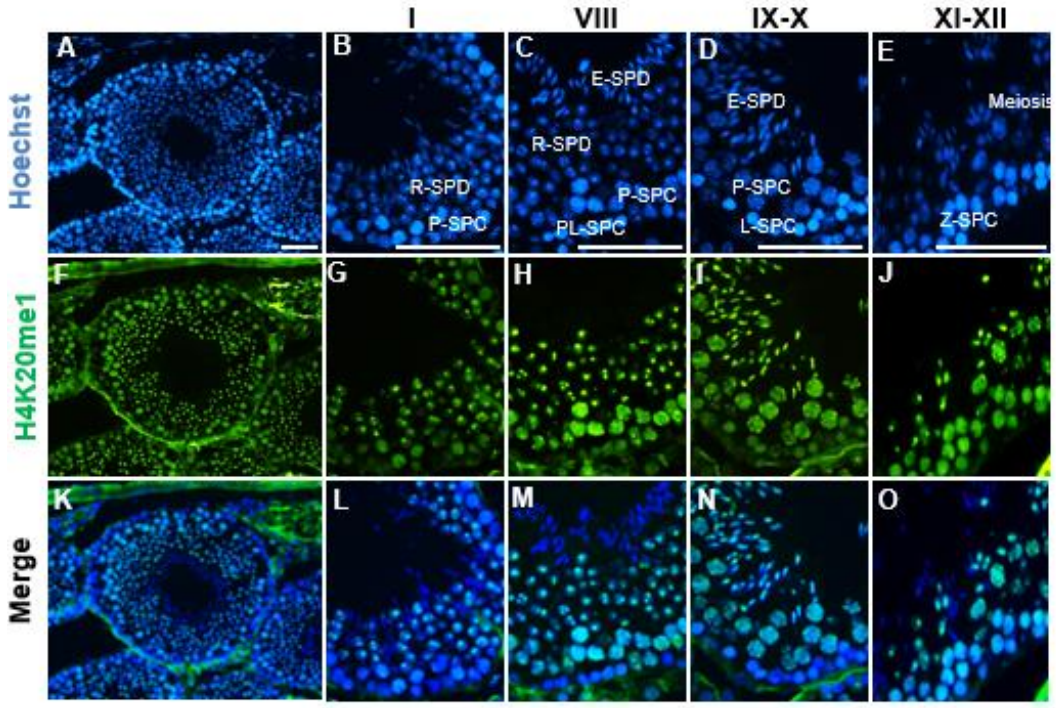

Fig. 4. The distribution of mono-methylated H4K20 in the seminiferous tubules. The distributions of nucleus (Blue: A-E), H4K20me1 (Green: F-J), and merged images (bottom panel: K-O) at stages I, VIII, IX-X, and XI-XII are shown. PL-SPC, preleptotene spermatocyte; L-SPC, leptotene spermatocyte; Z-SPC, zygotene spermatocyte; P-SPC, pachytene spermatocyte; R-SPD, round spermatid; E-SPD, elongated spermatid. Scale bars = 20μm.

CHAPTER III

RSBN1 exhibits demethylation function on both tri-methylation and di-methylation of H4K20 in round spermatids.

Introduction

In mammals, a number of enzymes regulate H4K20 methylation. To date, three methyltransferases (PR-SET7/SETD8/KMT5A, SUV420H1/KMT5B, and SUV420H2/KMT5C) have been implicated in mono-, di-, and tri-methylation of H4K20 (Nishioka *et al*., 2002; Pannetier *et al*., 2008; Rice *et al.*, 2002). PR-SET7 can catalyze only the mono-methylation of H4K20, while SUV420H1/KMT5B and SUV420H2/KMT5C can catalyze di- and tri-methylation of H4K20. On the other hand, four demethylases (LSD1n, KDM7B/PHF8, hHR23, and KDM9/DPY-21/RSBN1) that can demethylate methylated H4K20 have been reported (Brejc *et al*., 2017; Cao *et al*., 2020; Liu *et al*., 2010; Wang *et al*., 2015). Among them, PHF8 and LSD1n demethylates mono-methylated H4K20, whereas RSBN1 can convert di-methylation of H4K20 to mono-methylation but cannot demethylate mono-methylated and tri-methylated forms of H4K20. To date, hHR23 is the only catalyst that can demethylate mono-, di-, and tri-methylated H4K20 (Cao *et al*., 2020). Although H4K20 methyltransferases or H4K20 demethylases are shown to play a role in mammalian development, their roles during spermatogenesis still remain unclear (Malik *et al*., 2017; Wang *et al*., 2015; Xiong *et al*., 2013).

Among the H4K20 methylation modifiers, RSBN1/KDM9 might be an H4K20 demethylase, but its catalytic activity was only analyzed with partial RSBN1 ($RSBN1^{350-795}$) in the previous study (Brejc *et al*., 2017). It is not clear whether full length RSBN1 ($RSBN1^{1-795}$) can demethylate the tri-methylated form of H4K20. Here, I examined the demethylation function of full length RSBN1 ($RSBN1^{1-795}$) and compared dynamic changes of H4K20 methylation and RSBN1 localization patterns during spermatogenesis. The results implicated that the expression of RSBN1 is closely related to the distribution of three types of H4K20 methylation during spermiogenesis, which may indicate that RSBN1 plays important roles during the late stages of germ cell differentiation.

Materials and Methods

Cell culture and Transfection

The open reading frame (ORF) sequences of green fluorescence protein (GFP) was subcloned into pCS2-F vector, which contains RSBN1 ORF and a C-terminal FLAG tag sequence, by In-fusion HD cloning kit (Takara) according to the manufacturer's instruction. Primers that are used to amplify GFP and vector were listed in Table 1. Hela cells were maintained in Dulbecco's modified Eagle Medium (Thermo scientific) supplemented with 10% fetal calf serum (SIGMA), 1% glutamine (WAKO), and 1% penicillin-streptomycin (WAKO) at 37 ˚C in a humidified 5% CO_2 in air. 1-10 μg plasmids were transfected to Hela cells using Screen*Fect* A *plus* reagent (WAKO) following manufacturer's instruction. Cells were cultured for 24 hours and re-seeded onto poly-L-lysine coated coverslips.

Immunostaining

At 48 hours after transfection, Hela cells were fixed by 4% paraformaldehyde in PBS, washed, and immunostained by the methylated H4K20 antibodies before examination by fluorescence microscopy. Untransfected HeLa cells were used as control. To compare localization of RSBN1 and methylated H4K20 in the seminiferous tubules, double-immunostaining was carried out. Frozen sections that have been fixed and permeated were incubated with two primary antibodies diluted 1:1,000 with 3% BSA-PBS blocking buffer for overnight at 4˚C, followed by incubation with secondary

antibodies for one hour at room temperature. The primary antibodies were anti-RSBN1 (SCRUM Inc.), anti-H4K20me1 (GeneTex), anti-H4K20me2 (GeneTex), and anti-H4K20me3 (Abcam), and two secondary antibodies were Alexa 555-conjugated donkey anti-rabbit IgG and Alexa 488-conjugated goat anti-mouse IgG (both from Invitrogen).

Histone extraction and SDS-PAGE

For histone extraction, Hela cells were electroporated by the pCS2F-GFP-RSBN1 using NEPA21 (Nepa Gene) according to manufacturer's instruction. After 48 hours, histone proteins were extracted according to the procedure described before (Iwamori *et al*., 2011). The nuclear fraction was collected after cell lysis in the following buffer: 100mM Tris/HCl [pH 7.5], 1.5M NaCl, 1.5mM $MgCl_2$, 0.65% NP-40, and protease inhibitor cocktail. Histone proteins were extracted from the nuclear fraction by treatment with 0.2M H_2SO_4, followed by trichloro-acetic acid agglutination. Histone proteins were then analyzed by SDS-PAGE and the gel was stained by Coomassie blue solution at room temperature for 2 hours and decolorated by decoloring solution which contains 50% deionized water, 40% methanol, and 10% glacial acetic acid.

Immunoblotting and Band analysis

Extracted histone proteins of Hela cells were processed to immunoblot analysis. To examine RSBN1 demethylation function, amounts of methylated H4K20 in each group were compared by quantification of band densities by Quantity One software

(Bio-Rad). the relative fold change of histone of RSBN1-transfected cells compared to control cells was presented as the mean ± SEM. Primary antibodies were anti-histone H4 (Millpore) and other H4K20 methylated antibodies that were described above. Secondary antibodies were goat anti-rabbit IgG-HRP or goat anti-mouse IgG-HRP (both from Bio-Rad).

Results and Discussion

To evaluate the demethylating function of mouse RSBN1 on mono-, di-, and tri-methylation of H4K20, RSBN1 was expressed in HeLa cells, and the methylation intensity of each histone H4 lysine 20 was examined. Here, the plasmid vector pCS2-RSBN1-GFP, which contains a GFP ORF at the C-terminus of RSBN1, was constructed and transfected in HeLa cells (Fig 1). After transfection for 48h, RSBN1 was mainly localized in the nucleus but not in the cytoplasm of HeLa cells. Immunostaining results indicated that the fluorescence intensity of H4K20me3 and H4K20me2 in HeLa cells significantly decreased after RSBN1 expression, whereas that of H4K20me1 increased in RSBN1-expressing cells (Fig 2A). Histone proteins were extracted from HeLa cells, and the purification of histone proteins was confirmed by SDS-PAGE analysis (Fig 2B). Immunoblotting results indicated that the intensity of H4K20me3 and H4K20me2 bands in RSBN1-expressing cells decreased by 0.28 ± 0.2-fold and 0.58 ± 0.31-fold, respectively, whereas that of H4K20me1 increased by 1.61 ± 0.18-fold in RSBN1-expressing cells (Fig 2C). These results suggested that RSBN1 can demethylate H4K20me2 and H4K20me3 to H4K20me1.

Furthermore, to examine the relationship between RSBN1 and methylated H4K20 in the seminiferous tubules, their distribution was determined and compared. First, I compared the localization of RSBN1 and methylated H4K20 in elongated spermatids. The results suggested that RSBN1 staining intensity was strong in the cytoplasm of elongated spermatids at stage VII, but signals of three methylated H4K20 and RSBN1

in the nucleus of elongated spermatids were not detected (Fig 3A), suggesting that histones in elongated spermatids could be replaced by protamines at that stage. Therefore, RSBN1 in elongated spermatids may play other roles that are not related to histone demethylation. Although RSBN1 might be involved in the formation of subcellular functions, owing to being evenly distributed in elongated spermatids (Fig 3A), the specific localization of RSBN1 in organelles such as the acrosome, centriole, mitochondria, and flagellum were not determined in the present study. Additionally, it is necessary to identify interactive partners of RSBN1, which could be useful for us to comprehend the role of RSBN1 in the cytoplasm.

Next, the distribution of RSBN1 and methylated H4K20 was compared in RSBN1-positive round spermatids. Immunostaining results suggested that H4K20me3 and H4K20me2 were not present in RSBN1-positive round spermatids, but H4K20me1 was colocalized with RSBN1 (Fig 3B). The distribution of methylated H4K20 in RSBN1-expressing HeLa cells and round spermatids exhibited the same pattern, which strongly suggested that RSBN1 demethylates H4K20me3 and H4K20me2 into H4K20me1.

The demethylation function of RSBN1 examined in the previous report using partial amino acids of RSBN1 ($RSBN1^{350-795}$) showed the demethylation activity for H4K20me2 but not H4K20me3 (Brejc *et al*., 2017). In this study, the full-length amino acid sequence of RSBN1 ($RSBN1^{1-795}$) was used to verify the demethylation activity of RSBN1. The N-terminal region of RSBN1 ($RSBN1^{1-350}$) might increase the substrate recognition activity of RSBN1 or might be able to interact with other components to demethylate H4K20me3. As shown in our immunostaining results (Fig. 3), H4K20me3

signal was not detected in nucleus of round spermatids at stage VII in which RSBN1 was expressed. Thus, RSBN1 acts as a demethylase for both H4K20me2 and H4K20me3. Although no jmjC domain and PHD finger were found in the RSBN1 protein sequence, several sites including H582, D584, and H685, are conserved in mouse and *C. elegans*, which play critical roles in demethylase activity because they can interact with Fe^{2+} and α-KG (Brejc *et al*., 2017).

To date, several modifiers of H4K20 methylation have been found, but little is known about their expression and function during spermatogenesis. Recently, two homologs of yeast Rad23 (hHR23A and hHR23B) were reported as a demethylase for tri-, di-, and mono-methylated H4K20 (Cao *et al*., 2020). Theoretically, if hHR23A and hHR23B are expressed in round spermatids, mono-methylated H4K20 would disappear. However, strong H4K20me1 signals were observed in round spermatids, suggesting that H4K20me1 demethylase could not be expressed in round spermatids and that HR23s might not be involved in the regulation of methylated H4K20 during spermatogenesis. Thus, RSBN1 could be solely responsible for regulating H4K20 demethylation and generating the specific methylation patterns in round spermatids.

Results in this study suggested that RSBN1 can convert H4K20me3 and H4K20me2 into H4K20me1 but cannot demethylate H4K20me1. Given that methylated H4K20 is critical for genome integrity, chromatin remodeling, and transcriptional (Jørgensen *et al*., 2013; Pei *et al*., 2011; Schotta *et al.*, 2004; Shoaib *et al*., 2018), the regulation of methylated H4K20 could be essential for spermatogenesis. H4K20me3 marks pericentric heterochromatin and silences repetitive DNA and

transposons (Phalke *et al*., 2009; Schotta *et al*., 2004). Therefore, demethylation of H4K20me3 by RSBN1 could be a critical step for removing heterochromatin region prior to the histone removal.

In a previous report, DPY-21-mediated H4K20me1 was found to be involved in X-chromosome inactivation and to localize in compacted chromatin regions of *C. elegans*, to regulate X-dosage compensation (Brejc *et al*., 2017; Kramer *et al*., 2015; Vielle *et al*., 2012; Wells *et al*., 2012). Repressing effects of H4K20me1 on transcription and the results that H4K20me1 was intensive in spermatids at the steps 1-10 suggested that RSBN1 could repress transcription during spermiogenesis (Milite *et al*., 2016; Myers *et al.*, 2020; Kapoor-Vazirani *et al.*, 2014; Trojer *et al*., 2007). Otherwise, RSBN1-dependent accumulation of H4K20me1 in spermatids could be involved in chromatin compaction during the transformation of round spermatids to elongated spermatids, since chromatin condenses during this transformation process. Therefore, RSBN1, as a hallmark of spermiogenesis, needs to be thoroughly studied how it modifies the structure of chromatin in round spermatids and regulates the transcription in germ cell differentiation.

Table. 1. The primer sequences used for construction of recombinant plasmids in this study.

Name	Forward Primer	Reverse primer
GFP	CCAAGCACTCCTGTGATGGTGAGCAAGGGCGAGGA	GTCGTCCTTGTAGTCCTTGTACAGCTCGTCCATGC
pCS2-F	CACAGGAGTGCTTGGATGTG	GACTACAAGGACGACGATGACA

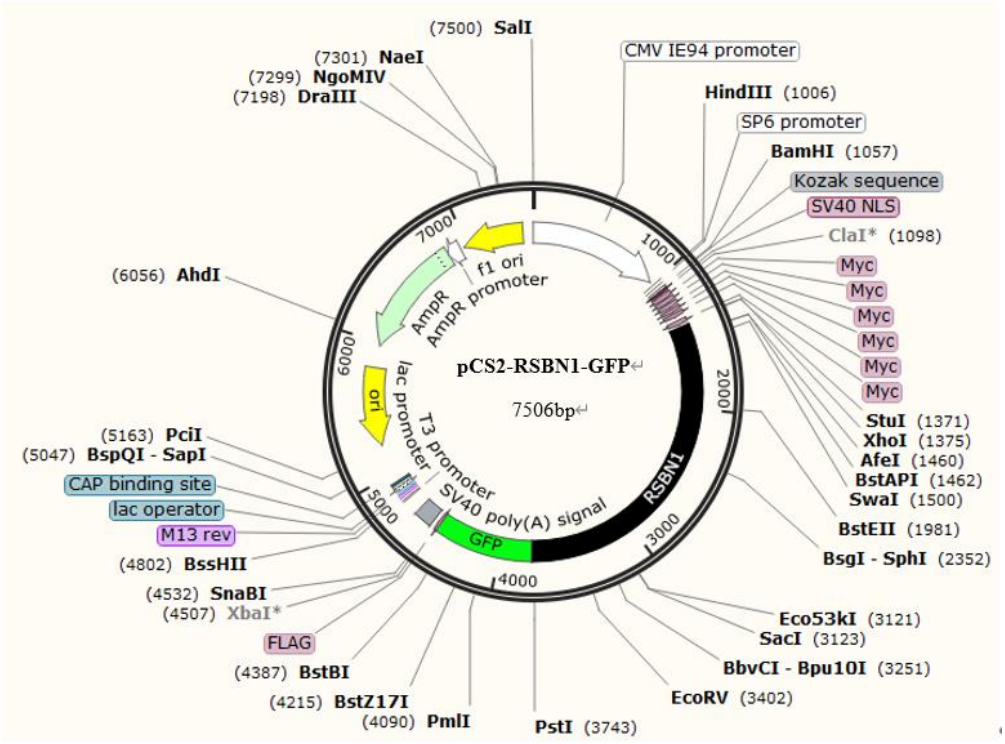

Fig. 1. Information of recombinant plasmid pCS2-RSBN1-GFP. ORF of GFP was subcloned in pCS2-RSBN1-F vector through homologous recombination.

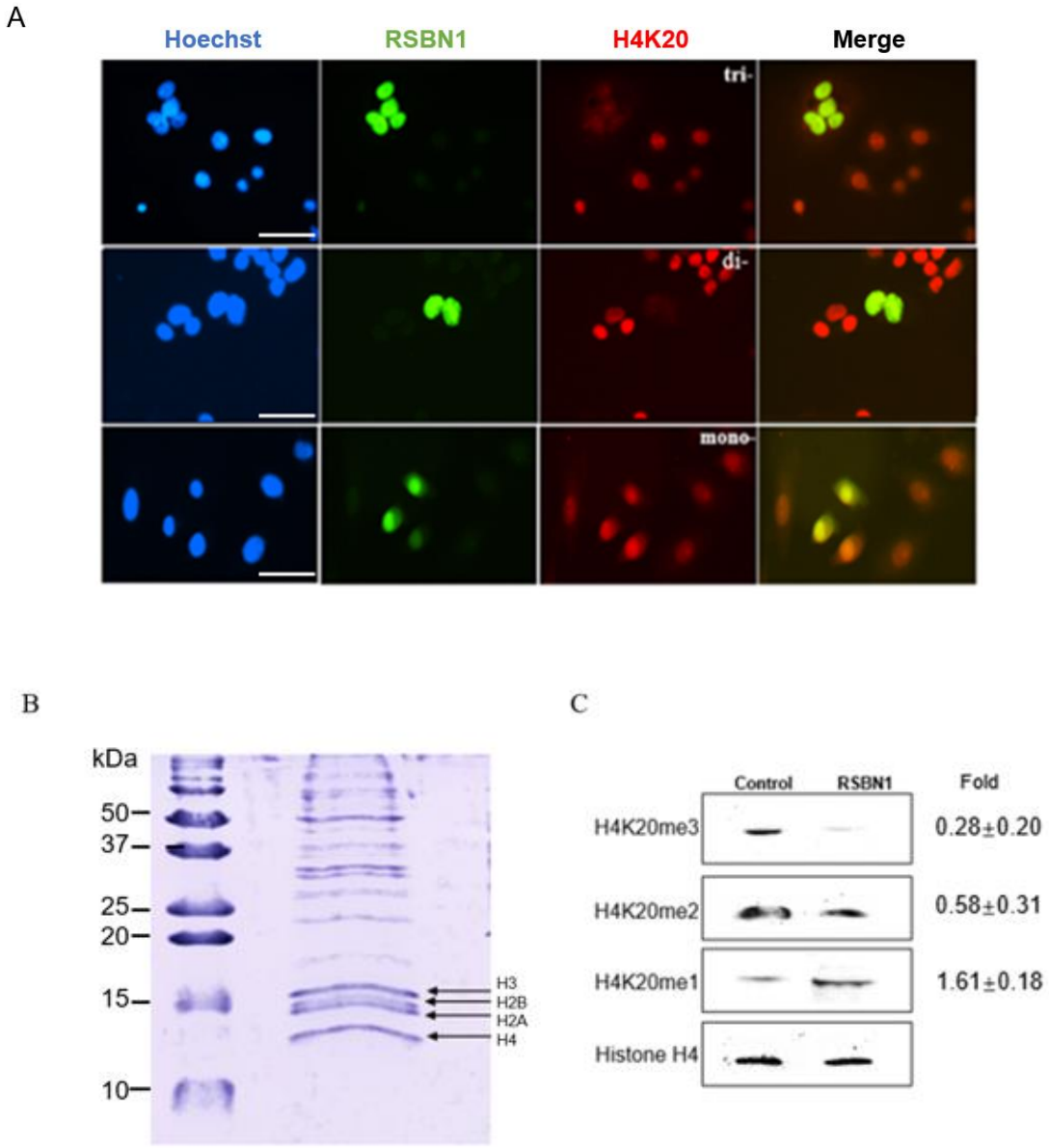

Fig. 2. Demethylation activity of RSBN1. (A) Tri-methylated, di-methylated, and mono-methylated H4K20 of RSBN1-positive Hela cells were stained by corresponding antibodies. Nucleus of Hela cell (blue), RSBN1 (green) and methylated H4K20 (red) are shown. Scale bars = 20μm. (B) Four bands of Hela cell histone proteins are shown by SDS-PAGE. (C) Immunoblot results of methylated H4K20 in non-transfected cells (control) and transfected cells (RSBN1). Values of relative fold change of band density

(RSBN1/Control) are shown at right of each images.

A

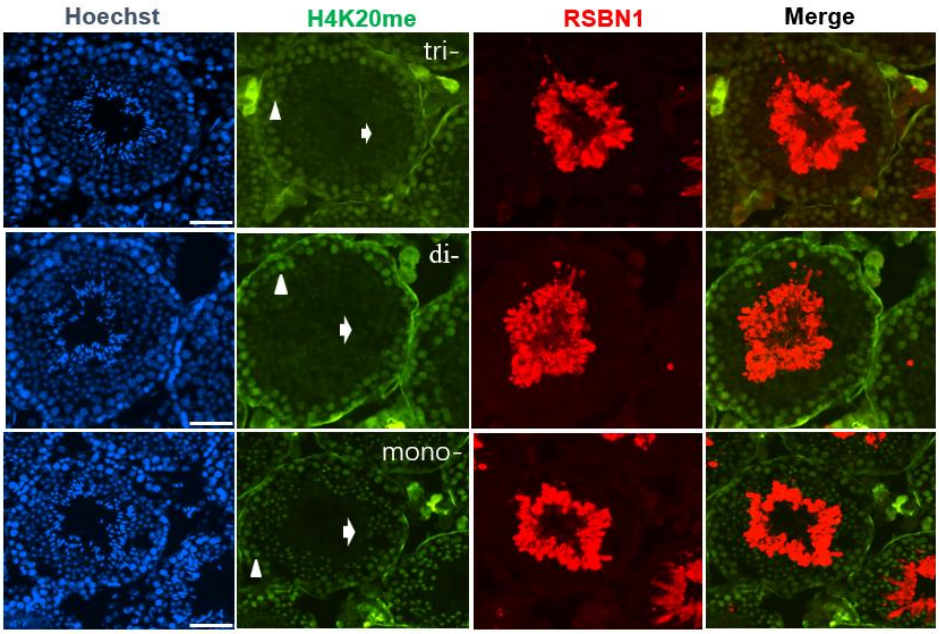

B

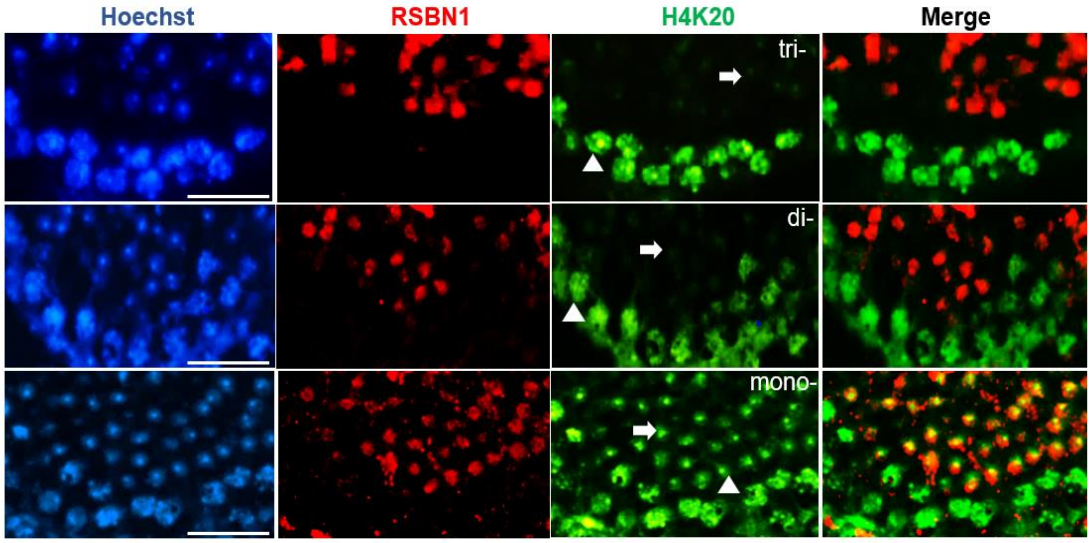

Fig. 3. Distributions of methylated H4K20 and RSBN1 in the stage VII of the seminiferous tubule. (A) The comparative distribution of RSBN1 and methylated H4K20 in elongated spermatids. The nucleus (blue), RSBN1 (red), methylated H4K20 (green), and merged images (right panel) are shown. Triangle and arrowhead represent

pachytene spermatocytes and elongated spermatids respectively. (B) The comparative distribution of RSBN1 and methylated H4K20 in round spermatids. The nucleus (blue), RSBN1 (red), methylated H4K20 (green), and merged images (right panel) are shown. Triangle and arrowhead represent pachytene spermatocytes and round spermatids respectively. Scale bars=20μm.

CONCLUSION

In Chapter I, the expression of RSBN1 in different tissues was examined. In addition to testis, RSBN1 was expressed in brain and ovary. Moreover, the localization of RSBN1 in both testes and ovaries was explored using a newly developed antibody specific to RSBN1. In contrast to the previous report in which RSBN1 was specifically expressed in testis and was localized only in the nucleus of round spermatids, the results in this study showed that RSBN1 was not testis-specific and was localized in both elongated and round spermatids in the testis. Furthermore, RSBN1 in the mouse ovary was expressed in the cytoplasm of stromal cells but not in oocytes, suggesting that RSBN1 could have different roles between male and female germ cell differentiation. Thus, our results redefined the expression and the distribution of RSBN1 in the mouse.

In Chapter II, the status of methylated H4K20 during spermatogenesis was identified by immunostaining, and methylated H4K20 was re-confirmed to be changed dynamically during spermatogenesis. The results indicated that methylated H4K20 was precisely regulated during spermatogenesis, although the roles of methylated H4K20 during spermatogenesis still remain to be elucidated.

In Chapter III, the demethylation function of full-length RSBN1 (RSBN1$^{1\text{-}795}$) was analyzed, and it was revealed that RSBN1 could demethylate both H4K20me3 and H4K20me2 in contrast to the previous report. In addition, the comparison between the distribution of RSBN1 and methylated H4K20 during spermatogenesis indicated that RSBN1 could be an important demethylase that constructs the specific distribution

pattern of methylated H4K20 at post-meiotic stages. Since methylated H4K20 is essential for genomic integrity, chromosome compaction, and transcriptional repression, RSBN1 could be responsible for the spermatogenesis through the regulation of H4K20 methylation. Thus, novel expression and function of RSBN1 revealed in this study could be useful to comprehend epigenetic regulation of spermatogenesis. The mechanism of RSBN1-mediated regulation of germ cell differentiation via H4K20 demethylation merits further investigation.

REFERENCES

Ahmed EA, Alzahrani AM, Scherthan H. Parp1-Dependent DNA Double-Strand Break Repair in Irradiated Late Pachytene Spermatocytes. DNA Cell Biol. 2021 Feb; 40(2): 209-218. doi:10.1089/dna.2020.5727.

Balakrishnan L, Milavetz B. Decoding the histone H4 lysine 20 methylation mark. Crit Rev Biochem Mol Biol. 2010 Oct; 45(5): 440-52. doi:10.3109/10409238.2010.504700.

Bannister AJ, Kouzarides T. Regulation of chromatin by histone modifications. Cell Research. 2011 Mar; (3): 381-95. doi:10.1038/cr.2011.22.

Beck DB, Oda H, Shen SS, Reinberg D. PR-Set7 and H4K20me1: at the crossroads of genome integrity, cell cycle, chromosome condensation, and transcription. Genes Dev. 2012 Feb; 26(4): 325-37. doi:10.1101/gad.177444.111.

Blendy JA, Kaestner KH, Weinbauer GF, Nieschlag E, Schutz G. Severe impairment of spermatogenesis in mice lacking the CREM gene. Nature. 1996 Mar; 380(6570): 162-5. doi:10.1038/380162a0.

Benetti R, Gonzalo S, Jaco I, Schotta G, Klatt P, Jenuwein T, Blasco MA. Suv4-20h deficiency results in telomere elongation and derepression of telomere recombination.

J Cell Biol. 2007 Sep; 178(6): 925-36. doi:10.1083/jcb.200703081.

Brejc K, Bian Q, Uzawa S, Wheeler BS, Anderson EC, King DS, Kranzusch PJ, Preston CG, Meyer BJ. Dynamic Control of X-Chromosome Conformation and Repression by a Histone H4K20 Demethylase. Cell. 2017 Sep; 171(1): 85–102. doi:10.1016/j.cell.2017.07.041.

Brustel J, Kirstein N, Izard F, Grimaud C, Prorok P, Cayrou C, Schotta G, Abdelsamie AF, Déjardin J, Méchali M, Baldacci G, Sardet C, Cadoret JC, Schepers A, Julien E. Histone H4K20 tri-methylation at late-firing origins ensures timely heterochromatin replication. EMBO J. 2017 Sep; 36(18): 2726-2741. doi:10.15252/embj.201796541.

Cao X, Chen Y, Wu B, Wang X, Xue H, Yu L. Histone H4K20 Demethylation by Two hHR23 Proteins. Cell Rep. 2020 Mar 24; 30(12): 4152-4164. doi:10.1016/j.celrep.2020.03.001.

Delaval K, Govin J, Cerqueira F, Rousseaux S, Khochbin S, Feil R. Differential histone modifications mark mouse imprinting control regions during spermatogenesis. EMBO J. 2007 Feb; 26(3): 720-9. doi:10.1038/sj.emboj.7601513.

Endo T, Mikedis MM, Nicholls PK, Page DC, de Rooij DG. Retinoic Acid and Germ Cell Development in the Ovary and Testis. Biomolecules. 2019 Nov; 9(12): 775.

doi:10.3390/biom9120775.

Fang J, Feng Q, Ketel CS, Wang H, Cao R, Xia L, Erdjument-Bromage H, Tempst P, Simon JA, Zhang Y. Purification and functional characterization of SET8, a nucleosomal histone H4-lysine 20-specific methyltransferase. Curr Biol. 2002 Jul; 12(13): 1086-99. doi:10.1016/s0960-9822(02)00924-7.

Fice HE, Robaire B. Telomere dynamics throughout spermatogenesis. Genes (Basel). 2019 Jul; 10(7): 525. doi:10.3390/genes10070525.

Greer EL, Shi Y. Histone methylation: A dynamic mark in health, disease, and inheritance. Nat Rev Genet. 2012 Apr; 13(5): 343-57. doi:10.1038/nrg3173.

Greeson NT, Sengupta R, Arida AR, Jenuwein T, Sanders SL. Dimethyl H4 Lysine 20 Targets the Checkpoint Protein Crb2 to Sites of DNA Damage. J Biol Chem. 2008 Nov; 283(48): 33168-74. doi:10.1074/jbc.M806857200.

Hess RA, De Franca LR. Spermatogenesis and cycle of the seminiferous epithelium. Adv Exp Med Biol. 2008; 636: 1-15. doi:10.1007/978-0-387-09597-4_1.

Huang H, Lin S, Garcia BA, Zhao Y. Quantitative proteomic analysis of histone modifications. Chem Rev. 2015 Mar; 115(6): 2376-418. doi:10.1021/cr50049lu.

Isono M, Niimi A, Oike T, Hagiwara Y, Sato H, Sekine R, Yoshida Y, Isobe SY, Obuse C, Nishi R, Petricci E, Nakada S, Nakano T, Shibata A. BRCA1 Directs the Repair Pathway to Homologous Recombination by Promoting 53BP1 Dephosphorylation. Cell Rep. 2017 Jan; 18(2): 520-532. doi:10.1016/j.celrep.2016.12.042.

Iwamori N, Iwamori T, Matzuk MM. H3K27 demethylase, JMJD3, regulates fragmentation of spermatogonial cysts. PLoS One. 2013 Aug; 8(8): e72689. doi:10.1371/journal.pone.0072689.

Iwamori N, Zhao M, Meistrich ML, Matzuk MM. The testis-enriched histone demethylase, KDM4D, regulates methylation of histone H3 lysine 9 during spermatogenesis in the mouse but is dispensable for fertility. Biol Reprod. 2011 Jun; 84(6): 1225-34. doi:10.1095/biolreprod.110.088955.

Jiang JY, Macchiarelli G, Tsang BK, Sato E. Capillary angiogenesis and degeneration in bovine ovarian antral follicles. Reproduction. 2003; 125(2): 211–23.

Jørgensen S, Schotta G, Sørensen CS. Histone H4 Lysine 20 methylation: Key player in epigenetic regulation of genomic integrity. Nucleic Acids Res. 2013 Mar; 41(5): 2797–806. doi:10.1093/nar/gkt012.

Kalakonda N, Fischle W, Boccuni P, Gurvich N, Hoya-Arias R, Zhao X, Miyata Y,

Macgrogan D, Zhang J, Sims JK, Rice JC, Nimer SD. Histone H4 lysine 20 monomethylation promotes transcriptional repression by L3MBTL1. Oncogene. 2008 Jul; 27(31): 4293-304. doi:10.1038/onc.2008.67.

Kapoor-Vazirani P, Vertino PM. A dual role for the histone methyltransferase PR-SET7/SETD8 and histone H4 lysine 20 monomethylation in the local regulation of RNA polymerase II pausing. J Biol Chem. 2014 Mar; 289(11): 7425–7437. doi:10.1074/jbc.M113.520783.

Karachentsev D, Sarma K, Reinberg D, Steward R. PR-Set7-dependent methylation of histone H4 Lys 20 functions in repression of gene expression and is essential for mitosis. Genes Dev. 2005 Feb; 19(4): 431-5. doi:10.1101/gad.1263005.

Kasioulis I, Syred HM, Tate P, Finch A, Shaw J, Seawright A, Fuszard M, Botting CH, Shirran S, Adams IR, Jackson IJ, van Heyningen V, Yeyati PL. Kdm3a lysine demethylase is an Hsp90 client required for cytoskeletal rearrangements during spermatogenesis. Mol Biol Cell. 2014; 25(8): 1216-33. doi:10.1091/mbc.E13-08-0471.

Kohlmaier A, Savarese F, Lachner M, Martens J, Jenuwein T, Wutz A. A chromosomal memory triggered by Xist regulates histone methylation in X inactivation. PLoS Biol. 2004 Jul; 2(7): E171. doi:10.1371/journal.pbio.0020171.

Kouzarides T. Chromatin Modifications and Their Function. Cell. 2007 Feb; 128(4): 693-705. doi:10.1016/j.cell.2007.02.005.

Kramer M, Kranz AL, Su A, Winterkorn LH, Albritton SE, Ercan S. Developmental Dynamics of X-Chromosome Dosage Compensation by the DCC and H4K20me1 in C. elegans. PLoS Genet. 2015 Dec; 11(12): e1005698. doi:10.1371/journal.pgen.1005698.

Kumari S, Muthusamy S. SETD2 as a regulator of N6-methyladenosine RNA methylation and modifiers in cancer. Eur J Cancer Prev. 2020 Nov; 29(6): 556-564. doi:10.1097/CEJ.0000000000000587.

Lata I, Tiwari S, Gupta A, Yadav S, Yadav S. To Study the Vitamin D Levels in Infertile Females and Correlation of Vitamin D Deficiency with AMH Levels in Comparison to Fertile Females. J Hum Reprod Sci. 2017; 10: 86–90. doi:10.4103/jhrs.JHRS_105_16.

Li Z, Nie F, Wang S, Li L. Histone H4 Lys 20 monomethylation by histone methylase SET8 mediates Wnt target gene activation. Proc Natl Acad Sci U S A. 2011 Feb; 108(8): 3116-23. doi:10.1073/pnas.1009353108.

Liu W, Tanasa B, Tyurina OV, Zhou TY, Gassmann R, Liu WT, Ohgi KA, Benner C, Garcia-Bassets I, Aggarwal AK, Desai A, Dorrestein PC, Glass CK, Rosenfeld MG. PHF8 mediates histone H4 lysine 20 demethylation events involved in cell cycle

progression. Nature. 2010 Jul; 466(7305): 508-12. doi:10.1038/nature09272.

Luense LJ, Donahue G, Lin-Shiao E, Rangel R, Weller AH, Bartolomei MS, Berger SL. Gcn5-mediated histone acetylation governs nucleosome dynamics in spermiogenesis. Dev Cell. 2019 Dec; 51(6): 745-758.e6. doi:10.1016/j.devcel.2019.10.024.

Malik J, Lillis JA, Couch T, Getman M, Steiner LA. The Methyltransferase Setd8 Is Essential for Erythroblast Survival and Maturation. Cell Rep. 2017 Nov; 21(9): 2376-2383. doi:10.1016/j.celrep.2017.11.011.

Martin C, Zhang Y. The diverse functions of histone lysine methylation. Nat Rev Mol Cell Biol. 2005 Nov; 6(11): 838-49. doi:10.1038/nrm1761.

Milite C, Feoli A, Viviano M, Rescigno D, Cianciulli A, Balzano AL, Mai A, Castellano S, Sbardella G. The emerging role of lysine methyltransferase SETD8 in human diseases. Clin Epigenetics. 2016 Sep; 8: 102. doi:10.1186/s13148-016-0268-4.

Mohan C, Das C, Tyler J. Histone and Chromatin Dynamics Facilitating DNA repair. DNA Repair (Amst). 2021 Aug; 107: 103183. doi:10.1016/j.dnarep.2021.103183.

Morera L, Lübbert M, Jung M. Targeting histone methyltransferases and demethylases in clinical trials for cancer therapy. Clin Epigenetics. 2016 May; 8: 57.

doi:10.1186/s13148-016-0223-4.

Mosammaparast N, Shi Y. Reversal of histone methylation: biochemical and molecular mechanisms of histone demethylases. Annu Rev Biochem. 2010; 79: 155-79. doi:10.1146/annurev.biochem.78.070907.103946.

Myers JA, Couch T, Murphy Z, Malik J, Getman M, Steiner LA. The histone methyltransferase Setd8 alters the chromatin landscape and regulates the expression of key transcription factors during erythroid differentiation. Epigenetics Chromatin. 2020 Mar; 13(1): 16. doi:10.1186/s13072-020-00337-9.

Nantel F, Monaco L, Foulkes NS, Masquilier D, LeMeur M, Henriksen K, Dierich A, Parvinen M, Sassone-Corsi P. Spermiogenesis deficiency and germ-cell apoptosis in CREM-mutant mice. Nature. 1996 Mar; 380(6570): 159-62. doi:10.1038/380159a0.

Ng JM, Vrieling H, Sugasawa K, Ooms MP, Grootegoed JA, Vreeburg JT, Visser P, Beems RB, Gorgels TG, Hanaoka F, Hoeijmakers JH, van der Horst GT. Developmental Defects and Male Sterility in Mice Lacking the Ubiquitin-Like DNA Repair Gene mHR23B. Mol Cell Biol. 2002 Feb; 22: 1233–45. doi:10.1128/mcb.22.4.1233-1245.2002.

Nishimura H, L'Hernault SW. Spermatogenesis. Curr Biol. 2017; 27: R988–R994.

doi:10.1016/j.cub.2017.07.067.

Nishioka K, Rice JC, Sarma K, Erdjument-Bromage H, Werner J, Wang Y, Chuikov S, Valenzuela P, Tempst P, Steward R, Lis JT, Allis CD, Reinberg D. PR-Set7 is a nucleosome-specific methyltransferase that modifies lysine 20 of histone H4 and is associated with silent Chromatin. Mol Cell. 2002 Jun; 9(6): 1201–13. doi:10.1016/S1097-2765(02)00548-8.

Ohyama K, Ohta M, Hosaka YZ, Tanabe Y, Ohyama T, Yamano Y. Expression of anti-Müllerian hormone and its type II receptor in germ cells of maturing rat testis. Endocr J. 2015; 62(11): 997-1006. doi:10.1507/endocrj.EJ15-0370.

Ozturk S. Telomerase activity and telomere length in male germ cells. Biol Reprod. 2015 Feb; 92(2): 53. doi:10.1095/biolreprod.114.124008.

Pannetier M, Julien E, Schotta G, Tardat M, Sardet C, Jenuwein T, Feil R. PR-SET7 and SUV4-20H regulate H4 lysine-20 methylation at imprinting control regions in the mouse. EMBO Rep. 2008 Oct; 9(10): 998-1005. doi:10.1038/embor.2008.147.

Paquin KL, Howlett NG. Understanding the Histone DNA Repair Code: H4K20me2 Makes Its Mark. Mol Cancer Res. 2018 Sep; 16(9): 1335-1345. doi:10.1158/1541-7786.MCR-17-0688.

Parikh G, Varadinova M, Suwandhi P, Araki T, Rosenwaks Z, Poretsky L, Seto-Young D. Vitamin D regulates steroidogenesis and insulin-like growth factor binding protein-1 (IGFBP-1) production in human ovarian cells. Horm Metab Res. 2010 Sep; 42: 754–757. doi:10.1055/s-0030-1262837.

Payne C, Braun RE. Histone lysine trimethylation exhibits a distinct perinuclear distribution in Plzf-expressing spermatogonia. Dev Biol. 2006 May; 293(2): 461-72. doi:10.1016/j.ydbio.2006.02.013.

Pei H, Zhang L, Luo K, Qin Y, Chesi M, Fei F, Bergsagel PL, Wang L, You Z, Lou Z. MMSET regulates histone H4K20 methylation and 53BP1 accumulation at DNA damage sites. Nature. 2011 Feb; 470(7332): 124-8. doi:10.1038/nature09658.

Peters AH, O'Carroll D, Scherthan H, Mechtler K, Sauer S, Schöfer C, Weipoltshammer K, Pagani M, Lachner M, Kohlmaier A, Opravil S, Doyle M, Sibilia M, Jenuwein T. Loss of the Suv39h histone methyltransferases impairs mammalian heterochromatin and genome stability. Cell. 2001 Nov; 107(3): 323–37. doi:10.1016/S0092-8674(01)00542-6.

Phalke S, Nickel O, Walluscheck D, Hortig F, Onorati MC, Reuter G. Retrotransposon silencing and telomere integrity in somatic cells of Drosophila depends on the cytosine-5 methyltransferase DNMT2. Nat Genet. 2009 Jun; 41(6): 696-702. doi:10.1038/ng.360.

Probst AV, Santos F, Reik W, Almouzni G, Dean W. Structural differences in centromeric heterochromatin are spatially reconciled on fertilisation in the mouse zygote. Chromosoma. 2007 Aug; 116(4): 403-15. doi:10.1007/s00412-007-0106-8.

Qi HH, Sarkissian M, Hu GQ, Wang Z, Bhattacharjee A, Gordon DB, Gonzales M, Lan F, Ongusaha PP, Huarte M, Yaghi NK, Lim H, Garcia BA, Brizuela L, Zhao K, Roberts TM, Shi Y. Histone H4K20/H3K9 demethylase PHF8 regulates zebrafish brain and craniofacial development. Nature. 2010 Jul; 466(7305): 503-7. doi:10.1038/nature09261.

Redon C, Pilch D, Rogakou E, Sedelnikova O, Newrock K, Bonner W. Histone H2A variants H2AX and H2AZ. Curr Opin Genet Dev. 2002 Apr; 12(2): 162-9. doi:10.1016/s0959-437x(02)00282-4.

Rice JC, Nishioka K, Sarma K, Steward R, Reinberg D, David Allis C. Mitotic-specific methylation of histone H4 Lys 20 follows increased PR-Set7 expression and its localization to mitotic chromosomes. Genes Dev. 2002 Sep; 16(17): 2225-30. doi:10.1101/gad.1014902.

Russell LD, Ettlin RA, SinhaHikim AP, Clegg ED. Histological and histopathological evaluation of the testis. Cache River Press. 1990.

Schotta G, Lachner M, Sarma K, Ebert A, Sengupta R, Reuter G, Reinberg D, Jenuwein T. A silencing pathway to induce H3-K9 and H4-K20 trimethylation at constitutive heterochromatin. Genes Dev. 2004 Jun; 18(11): 1251–62. doi:10.1101/gad.300704.

Schotta G, Sengupta R, Kubicek S, Malin S, Kauer M, Callén E, Celeste A, Pagani M, Opravil S, De La Rosa-Velazquez IA, Espejo A, Bedford MT, Nussenzweig A, Busslinger M, Jenuwein T. A chromatin-wide transition to H4K20 monomethylation impairs genome integrity and programmed DNA rearrangements in the mouse. Genes Dev. 2008 Aug; 22(15): 2048-61. doi:10.1101/gad.476008.

Shirakata Y, Hiradate Y, Inoue H, Sato E, Tanemura K. Histone H4 Modification During Mouse Spermatogenesis. J Reprod Dev. 2014; 60(5): 383-7. doi:10.1262/jrd.2014-018.

Shoaib M, Walter D, Gillespie PJ, Izard F, Fahrenkrog B, Lleres D, Lerdrup M, Johansen JV, Hansen K, Julien E, Blow JJ, Sørensen CS. Histone H4K20 methylation mediated chromatin compaction threshold ensures genome integrity by limiting DNA replication licensing. Nat Commun. 2018 Sep; 9(1): 3704. doi:10.1038/s41467-018-06066-8.

Stillman B. Histone Modifications: Insights into Their Influence on Gene Expression. Cell. 2018 Sep; 175(1): 6-9. doi:10.1016/j.cell.2018.08.032.

Sun H, Shi Y, Shang Y, Chen X, Xia F. MicroRNA-378d inhibits Glut4 by targeting Rsbn1 in vitamin D deficient ovarian granulosa cells. Mol Med Rep. 2021 May; 23(5): 369. doi:10.3892/mmr.2021.12008.

Takahashi T, Tanaka H, Iguchi N, Kitamura K, Chen Y, Maekawa M, Nishimura H, Ohta H, Miyagawa Y, Matsumiya K, Okuyama A, Nishimune Y. Rosbin: a novel homeobox-like protein gene expressed exclusively in round spermatids. Biol Reprod. 2004 May; 70(5): 1485-92. doi:10.1095/biolreprod.103.026096.

Tanemura K, Ogura A, Cheong C, Gotoh H, Matsumoto K, Sato E, Hayashi Y, Lee HW, Kondo T. Dynamic rearrangement of telomeres during spermatogenesis in mice. Dev Biol. 2005 May; 281(2): 196–207. doi:10.1016/j.ydbio.2005.02.025.

Tjalsma SJD, Hori M, Sato Y, Bousard A, Ohi A, Raposo AC, Roensch J, Le Saux A, Nogami J, Maehara K, Kujirai T, Handa T, Bagés-Arnal S, Ohkawa Y, Kurumizaka H, da Rocha ST, Żylicz JJ, Kimura H, Heard E. H4K20me1 and H3K27me3 are concurrently loaded onto the inactive X chromosome but dispensable for inducing gene silencing. EMBO Rep. 2021 Mar; 22(3): e51989. doi:10.15252/embr.202051989.

Trojer P, Li G, Sims RJ, Vaquero A, Kalakonda N, Boccuni P, Lee D, Erdjument-Bromage H, Tempst P, Nimer SD, Wang YH, Reinberg D. L3MBTL1, a histone-methylation-dependent chromatin lock. Cell. 2007 Jun; 129(5): 915–928.

doi:10.1016/j.cell.2007.03.048.

Vielle A, Lang J, Dong Y, Ercan S, Kotwaliwale C, Rechtsteiner A, Appert A, Chen QB, Dose A, Egelhofer T, Kimura H, Stempor P, Dernburg A, Lieb JD, Strome S, Ahringer J. H4K20me1 Contributes to Downregulation of X-Linked Genes for C. elegans Dosage Compensation. PLoS Genet. 2012 Sep; 8(9): e1002933. doi:10.1371/journal.pgen.1002933.

Walport LJ, Hopkinson RJ, Schofield CJ. Mechanisms of human histone and nucleic acid demethylases. Curr Opin Chem Biol. 2012 Dec; 16(5-6): 525-34. doi:10.1016/j.cbpa.2012.09.015.

Wang H, Andoh K, Hagiwara H, Xiaowei L, Kikuchi N, Abe Y, Yamada K, Fatima R, Mizunuma H. Effect of adrenal and ovarian androgens on type 4 follicles unresponsive to FSH in immature mice. Endocrinology. 2001 Nov; 142(11): 4930-6. doi:10.1210/endo.142.11.8482.

Wang J, Telese F, Tan Y, Li W, Jin C, He X, Basnet H, Ma Q, Merkurjev D, Zhu X, Liu Z, Zhang J, Ohgi K, Taylor H, White RR, Tazearslan C, Suh Y, Macfarlan TS, Pfaff SL, Rosenfeld MG. LSD1n is a H4K20 demethylase regulating memory formation via transcriptional elongation control. Nat Neurosci. 2015 Sep; 18(9): 1256-64. doi:10.1038/nn.4069.

Wang Y, Jia S. Degrees make all the difference: the multifunctionality of histone H4 lysine 20 methylation. Epigenetics. 2009 Jul; 4(5): 273-6. doi:10.4161/epi.4.5.9212.

Wang Z, Zang C, Rosenfeld JA, Schones DE, Barski A, Cuddapah S, Cui K, Roh TY, Peng W, Zhang MQ, Zhao K. Combinatorial patterns of histone acetylations and methylations in the human genome. Nat Genet. 2008 Jul; 40(7): 897-903. doi:10.1038 /ng.154.

Wells MB, Snyder MJ, Custer LM, Csankovszki G. Caenorhabditis elegans Dosage Compensation Regulates Histone H4 Chromatin State on X Chromosomes. Mol Cell Biol. 2012 May; 32(9): 1710-9. doi:10.1128/MCB.06546-11.

Wu S, Li H, Wang L, Mak N, Wu X, Ge R, Sun F, Cheng CY. Motor Proteins and Spermatogenesis. Adv Exp Med Biol. 2021; 1288: 131-159. doi:10.1007/978-3-030-77 779-1_7.

Xiong K, Wu W, Wang X, Ma X, Chen J, Liu H. Mouse oocyte meiosis is disturbed by knockdown of Suv4-20h. Reprod Fertil Dev. 2013; 25(3): 503-10. doi:10.1071/RD12116.

ACKNOWLEDGMENT

As an international student, I spent a period of meaningful time in japan. Japan is a very beautiful country. I was very lucky to be admitted by Graduate school of Bioresource and Environment, Faculty of Agriculture, Kyushu University in 2017. Kyushu university is a famous national university in Japan and is known as its outstanding academic contributions in Japan even in the world. I thought it is very memorable to study in Japan for three years. Because I felt a different education environment and met so many excellent scholars, which broadened my vision.

First of all, I would like to thank Prof. Hiroshi Iida who gave me an opportunity to study in Laboratory of Zoology and helped me getting used to life in Japan. He is an interesting and wise teacher. He always gives us very helpful suggestion in our daily work. When I faced difficulties in my experiment, he always come up with solutions to help me solving problems.

During the three years, I really appreciate Prof. Naoki Iwamori who supported me a lot in my experiment and helped me solving a lot of problems in my research project when I was confronted with confusions and difficulties. He instructed me performing many experiments and learning theoretical knowledge, which will be very useful in my career. His profound insight and excellent academic consciousness helped me developing some special way of thinking. Under his supervision and instruction, I gained more knowledges in field of Developmental Biology.

I also would like to thank associate Prof. Tokuko Iwamori for her guidance on my

paper. She is a knowledgeable expert. During my publication of the paper, I encountered many difficult problems. She helped me modifying the paper so that my paper can be published smoothly. Like other Chinese students, I am honored to receive her guidance.

Then, I would like to extend my sincere gratitude to assistant Prof. Takane Kaneko, she is a very kind teacher. She provided me some reagents and experimental experiences which improved the progress of my research. In this work, she instructed me to purify the polyclonal antibody and told me many skills when I made testis frozen section. On the other hand, she helped me addressing many student daily works. As an international student, I was confused at sometimes by some management style or rules of University, she always explains every detail of rules to me or other foreign students very patiently.

Finally, I want to express heartfelt thanks to all students that I have communicated with in Lab, they are very friendly and kindhearted. Under their assistance, I had been successfully assimilated into the zoology laboratory.